bioRxiv preprint doi: https://doi.org/10.1101/2020.07.17.208132; this version posted July 17, 2020. The copyright holder for this preprint (which was not certified by peer review) is the author/funder, who has granted bioRxiv a license to display the preprint in perpetuity. It is made available under aCC-BY-NC-ND 4.0 International license.

Transcriptional Signatures of Synaptic Vesicle Genes Define Myotonic Dystrophy Type I Neurodegeneration

Antonio Jimenez-Marin[1,2], Ibai Diez[3,4,5], Garazi Labayru[6,7,8], Andone Sistiaga[6,7,8], Jorge Sepulcre[3,4,5], Adolfo Lopez de Munain[6,7,9,10,] and Jesus M. Cortes[1,11,12,*,§]*

1. Computational Neuroimaging Group, Biocruces-Bizkaia Health Research Institute. Barakaldo, Spain.

2. Biomedical Research Doctorate Program, University of the Basque Country (UPV/EHU). Leioa, Spain.

3. Department of Radiology, Division of Nuclear Medicine and Molecular Imaging, Massachusetts General Hospital and Harvard Medical School. Boston, United States of America.

4. Gordon Center for Medical Imaging, Department of Radiology, Massachusetts General Hospital and Harvard Medical School. Boston, United States of America.

5. Athinoula A. Martinos Center for Biomedical Imaging, Massachusetts General Hospital, Harvard Medical School. Boston, United States of America.

6. Neuroscience Area, Biodonostia Research Institute. San Sebastián, Spain.

7. Centro de Investigación Biomédica en Red sobre Enfermedades Neurodegenerativas (CIBERNED), Institute Carlos III. Madrid, Spain.

8. Personality, Assessment and Psychological Treatment Department; Psychology Faculty, University of the Basque Country (UPV/EHU). San Sebastian, Spain.

9. Neurology Department, Donostia University Hospital. Donostia-San Sebastian, Spain.

10. Neurosciences Department, University of the Basque Country (UPV/EHU). Donostia-San Sebastian, Spain.

11. Cell Biology and Histology Department, University of the Basque Country (UPV/EHU). Leioa, Spain.

12. IKERBASQUE, The Basque Foundation for Science. Bilbao, Spain.

* *Equal last-author contribution*

§ *Correspondence: jesus.m.cortes@gmail.com*

bioRxiv preprint doi: https://doi.org/10.1101/2020.07.17.208132; this version posted July 17, 2020. The copyright holder for this preprint (which was not certified by peer review) is the author/funder, who has granted bioRxiv a license to display the preprint in perpetuity. It is made available under aCC-BY-NC-ND 4.0 International license.

Abstract

Despite significant research, the biological mechanisms underlying the brain degeneration in Myotonic Dystrophy Type I (DM1) remain largely unknown. Here we have assessed brain degeneration by measuring the volume loss (VL) and cognitive deficits (CD) in two cohorts of DM1 patients, and associating them to the large-scale brain transcriptome maps provided by the Allen Human Brain Atlas (AHBA). From a list of preselected hypothesis-driven genes, three of them appear to play a major role in degeneration: dystrophin (*DMD)*, alpha-synuclein (*SNCA)* and the microtubule-associated protein tau (*MAPT)*. Moreover, a purely data-driven strategy identified gene clusters enriched for key biological processes in the central nervous system, such as synaptic vesicle recycling, localization, endocytosis and exocytosis, and the serotonin and dopamine neurotransmitter pathways. Therefore, by combining large-scale transcriptome interactions with brain imaging and cognitive function, we provide a new more comprehensive understanding of DM1 that might help define future therapeutic strategies and research into this condition.

bioRxiv preprint doi: https://doi.org/10.1101/2020.07.17.208132; this version posted July 17, 2020. The copyright holder for this preprint (which was not certified by peer review) is the author/funder, who has granted bioRxiv a license to display the preprint in perpetuity. It is made available under aCC-BY-NC-ND 4.0 International license.

Introduction

Myotonic Dystrophy type 1 (DM1) is a complex multisystem disease that affects skeletal muscles[1], the heart[2], lungs[3], endocrine system[4], the regulation of sleep cycles[5] and other aspects of brain activity[6]. Epidemiologically, DM1 is the most common adult-onset muscular dystrophy in humans, with a reported prevalence of 1/7,400 people worldwide[7] that is about three times higher in Gipuzkoa[8], Northern Spain (where this study was performed). Neuroimaging studies has shown the brain damage in DM1 patients, such as gray matter atrophy mainly affecting the frontal and parietal lobes[9] but also, in the hippocampus[10] and other subcortical structures[11]. More recent studies, also showed that DM1 produces atrophy along white-matter tracts[12,13], affecting the large-scale connectivity of the human brain.

Using an approach that combines magnetic resonance imaging (MRI) and large-scale brain transcriptomics, we aimed here to assess to what extent *the structural damage in the DM1 brain represents a neurogenetic signature.* In contrast to other neurodegenerative diseases in which a large number of candidate genes are implicated, for example about 700 genes in Alzheimer's Disease (AD)[14], DM1 is a monogenic disorder caused by a mutation in the gene encoding the myotonic dystrophy protein kinase (*DMPK*)[15]. However, although the disease is monogenic, its phenotype is mainly due to an abnormal activity of the RNA-binding protein muscleblind-like 1 and 2 genes (*MBNL1*, *MBNL2*)[16,17] and CUGBP which regulates the expression of many other genes, such as the chloride channel 1 gene (*CLCN1*) that regulates chloride conductance during muscle development[18], the insulin receptor gene (*INSR*)[19], the bridging integrator 1 gene (*BIN1*)[20] or other genes directly related to the main symptoms of the condition[21]. The symptomatology of DM1 is mainly associated to cognitive difficulties including visuospatial processing and executive functioning[22,23]. Strikingly, the *DMPK* pathogenic genotype has also been associated with other genes that encode proteins implicated in brain neurodegeneration, majorly to tau deposits[24], but also amyloid beta (Aβ)[25] or alpha synuclein[26,27]. Thus, it is suspected that the cognitive deficits and brain damage found in DM1 patients might present some similarities to that in other neurodegenerative diseases, although this issue has yet to be fully addressed.

bioRxiv preprint doi: https://doi.org/10.1101/2020.07.17.208132; this version posted July 17, 2020. The copyright holder for this preprint (which was not certified by peer review) is the author/funder, who has granted bioRxiv a license to display the preprint in perpetuity. It is made available under aCC-BY-NC-ND 4.0 International license.

Therefore, despite the monogenic origin of DM1, the gene-to-gene interactome scales up to implicate multiple systems in the brain and body. To date, a precise association between the entire transcriptome and the brain neurodegeneration and cognitive deterioration in DM1 patients remains unexplored.

Some studies have assessed the relationship between genetics and structural brain alterations in DM1, confirming that the number of pathogenic repeats of the cytosine-thymine-guanine (CTG) triplet in the DMPK gene (a parameter used to quantify the molecular severity of the disease) was associated with both stronger gray and white matter atrophy, and to the cognitive deficits of these patients[28,29]. Here, we performed an intersection analysis of neuroimaging phenotypes and the Allen Human Brain Atlas (AHBA) of large-scale transcriptional human data[30], following a similar methodology to that used previously[31–33]. Our hypothesis was that identifying the genes whose expression coincided more closely with the brain damage found in DM1 patients, we might better understand the gene relationships associated with the brain damage that arises in this pathology. Similarly, we also assessed the relationship between gene transcription in specific anatomical regions and the brain maps of cognitive deficits in these patients.

Methods

Participants, two cohorts

A total of N=95 subjects were recruited to a cross-sectional study, 35 of whom were DM1 patients who were treated at the Neurology Department of the Donostia University Hospital (Gipuzkoa, Spain), while 60 subjects participated as Healthy controls (HCs). All patients and HCs were recruited from the vicinity of the Donostia University Hospital, and the two groups were matched for age, gender and education. The imaging data from the DM1 patients and HCs was acquired at two different Institutions. At one, 19 DM1 patients (mean age 53.3 years [SD ±8.1 years]; 9 males, 10 females) and 29 HC (52.2 [±8.1] years; 12 males, 17 females) were examined and at the second, 16 DM1 patients (48.8 [±7.7] years; 7 males, 9 females) and 31 HC

bioRxiv preprint doi: https://doi.org/10.1101/2020.07.17.208132; this version posted July 17, 2020. The copyright holder for this preprint (which was not certified by peer review) is the author/funder, who has granted bioRxiv a license to display the preprint in perpetuity. It is made available under aCC-BY-NC-ND 4.0 International license.

(47.6 [± 7.6] years; 14 males, 17 females). For the mean values, and the comparisons between groups and cohorts see Tables 1 and S1.

The DM1 patients were only included if they had molecular confirmation of their DM1 diagnosis, indicating the expansion of hundreds to thousands of CTG repeats in the *DMPK* gene[15]. The diagnosis was obtained when patients were between 18 and 40 years old, and following the adult-onset proposed as the fourth outcome measure for myotonic dystrophy type 1 (OMMYD-4). Patients were excluded if at least one of the following criteria was met: congenital or pediatric disease onset; a history of a major psychiatric or somatic disorder in accordance with DSM-V criteria; acquired brain damage; alcohol or drug abuse; the presence of corporal paramagnetic devices like pacemakers or metal prosthesis that might compromise the MRI studies; and the presence of brain abnormalities that could affect the volumetric analysis. HCs satisfied the same exclusion criteria but the number of the CTG repeats in their *DMPK* gene ranged from 5 to 34[15]. DM1 patients were recruited from the Neuromuscular Unit in the Neurology Department of the Hospital Universitario Donostia, while HCs were recruited from their healthy relatives in whom in the *DMPK* expansion was excluded.

All participants were informed about the study and offered their signed their informed consent. The study was approved by the Ethical Committee of the Donostia University Hospital (code DMRM-2017-01) and it was carried out in accordance with the tenets for human research laid out in the Helsinki Declaration.

Demographic, clinical and neuropsychological variables

The demographic variables of the subjects recorded were their age, gender and years of education. The clinical variables were the CTG expansion size and Muscular Impairment Rating Scale (MIRS) score[34]. Neuropsychological variables corresponded to composite values from different cognitive domains obtained through a comprehensive neuropsychological evaluation performed by an experienced neuropsychologist who was blind to the patient's clinical condition

bioRxiv preprint doi: https://doi.org/10.1101/2020.07.17.208132; this version posted July 17, 2020. The copyright holder for this preprint (which was not certified by peer review) is the author/funder, who has granted bioRxiv a license to display the preprint in perpetuity. It is made available under aCC-BY-NC-ND 4.0 International license.

(CTG expansion size and MIRS results). The neuropsychological assessment included several subtests from the Wechsler Adult Intelligence Scale III (WAIS III)[35], including: Digit span, Vocabulary, Block design, Object assembly, Arithmetic, and Similarities. Other cognitive tests used were: Stroop, California Computerized Assessment Package (CALCAP), Raven's progressive matrices, Rey Auditory Verbal Learning Test (RAVLT)[36], Word Fluency[37,38], Rey-Osterrieth Complex Figure test (ROCF)[39] and Benton's Judgement of Line Orientation[40]. The patients' raw scores were converted into standardized t-values based on the normative scores for the Spanish population in each test. Finally, the different neuropsychological scores were reduced into six different domains: visuospatial (Block design and ROCF copy), verbal memory (RAVLT immediate recall, RAVLT delayed recall, Total RAVLT), attention (Digit span, STROOP word, STROOP color, Simple Reaction Time (RT), election RT, Sequential 1 RT, Sequential 2 RT), executive functioning (Total RAVEN, semantic fluency, phonemic fluency, STROOP color-word, STROOP interference), visual memory (ROCF delayed recall), and intelligence.

MRI acquisition and preprocessing

For the first cohort, MRI was conducted on a 3 Tesla scanner (TrioTim, Siemens) using a high-resolution 3D sequence of magnetization-prepared rapid acquisition with gradient echo (MPRAGE) and applying the following parameters: Sagittal 3D T1 weighted acquisition, TR = 2300 ms, TE = 2.86 ms, inversion time = 900 ms, flip angle = 9 deg, matrix = 192 x 192 mm^2, slice thickness = 1.25 mm, voxel dimensions = 1.25 x 1.25 x 1.25 mm^3, NSA = 1, slices = 144, no gap, total scan duration = 7 min and 22 sec. For the second cohort, MRI was conducted on a 1.5 Tesla scanner (Achieva Nova, Philips), using a high-resolution volumetric turbo field echo (TFE) sequence with the following parameters: Sagittal 3D T1 weighted acquisition, TR = 7.2 ms, TE = 3.3 ms, inversion time = 0 ms, flip angle = 8 deg, matrix = 256 x 232 mm^2, slice thickness = 1mm, voxel dimensions = 1 x 1 x 1 mm^3, NSA = 1, slices = 160, no gap, total scan duration = 5 min 34 sec.

bioRxiv preprint doi: https://doi.org/10.1101/2020.07.17.208132; this version posted July 17, 2020. The copyright holder for this preprint (which was not certified by peer review) is the author/funder, who has granted bioRxiv a license to display the preprint in perpetuity. It is made available under aCC-BY-NC-ND 4.0 International license.

To perform voxel-based gray matter (GM) morphometric comparisons between the subjects, DM1 and HCs, we performed Voxel-Based Morphometry (VBM) following a procedure similar to that used previously[41,42], an optimized VBM protocol[43] carried out with the FSL v6.01 software. First, skull-removal was performed, followed by GM segmentation and registration to the MNI 152 standard space using non-linear registration[44]. The resulting images were averaged and flipped along the x-axis to create a left-right symmetric, study-specific GM template. Second, all native GM images were non-linearly registered to this study-specific template and "modulated" to correct for local expansion (or contraction) due to the non-linear component of the spatial transformation. The modulated GM images were then smoothed with an isotropic Gaussian kernel at sigma = 3 and finally, the partial gray matter volume estimates normalized to the subject's head size were compared.

Imaging statistical analysis

For the VBM analyses, a generalized lineal model was fitted for each voxel and image using the FSL software, controlling for age and head size with two different contrasts: DM1 < HC and DM1 > HC. All the results were obtained with two-tailed tests, correcting for multiple comparisons using the Monte Carlo simulation clusterwise correction implemented in the AFNI v19.3.00 software, and using 10,000 iterations to estimate the probability of false positive clusters with a p-value < 0.05. Each cohort was analyzed separately and in combination, as explained below, although statistical comparisons between the two cohorts were not performed.

Transcriptomics brain maps

To build brain maps of transcription we took advantage of the publicly available data from the Allen Human Brain Atlas (AHBA – http://human.brain-map.org/)[30]. The dataset consisted of MRI images and a total of 58,692 microarray-based transcription profiles of about 20,945 genes sampled over 3,702 different regions across the brains of six humans. To pool all the transcription data into a single brain template, we followed a similar procedure to that employed elsewhere[45]. First, to re-annotate the probes to genes we made use of the re-annotator toolkit[46].

bioRxiv preprint doi: https://doi.org/10.1101/2020.07.17.208132; this version posted July 17, 2020. The copyright holder for this preprint (which was not certified by peer review) is the author/funder, who has granted bioRxiv a license to display the preprint in perpetuity. It is made available under aCC-BY-NC-ND 4.0 International license.

Second, we removed those probes with insufficient signal by looking at the sampling proportion (SP), which was calculated for each brain as the ratio between the samples with a signal greater than the background noise divided by the total number of samples. Probes with a SP lower than 70% in any of the six brains were removed from the analysis, thereby ensuring sufficient sampling power in all the brains. After that, we chose the value of the probe for each gene with the maximum differential stability (DS), accounting for the reproducibility of gene expression across brain regions and individuals, and calculated using spatial correlations similar to those employed previously[47]. For this the Automated Anatomical Labelling (AAL) atlas was used[48] from which the cerebellum was excluded, resulting in 90 different anatomical regions*. Finally, to remove the inter-subject differences the transcription values for each gene and brain were transformed into Z-scores, and pooled together from the six different brains, obtaining a single map using the MNI coordinates provided in the dataset. Finally, to eliminate the spatial dependencies of the transcription values at the sampling sites (that is, to correct for the fact that nearest sites have more correlated transcription), we finally obtained a single transcription value for each region in the AAL atlas by calculating the median of all the values belonging to the given region.

Association between volume loss and transcriptomics

Volume loss (VL) was defined as the t-statistic resulting from the group comparison DM1 < HC. To associate VL with transcriptomics, we transformed the t-statistics map to the same AAL atlas as that used for the transcription values, calculating the median of the t-statistics between all values in each region. For each gene, we calculated a similarity index using the Pearson correlation coefficient between VL and transcriptomics, the two variables represented in vectors

* AAL regions were eroded with a Gaussian kernel with a full width at half maximum (FWHM) equal to 2 mm, thereby eliminating false-positive sampling sites, i.e.: those that do not belong to the region of interest but to one in the neighborhood.

bioRxiv preprint doi: https://doi.org/10.1101/2020.07.17.208132; this version posted July 17, 2020. The copyright holder for this preprint (which was not certified by peer review) is the author/funder, who has granted bioRxiv a license to display the preprint in perpetuity. It is made available under aCC-BY-NC-ND 4.0 International license.

with a dimension equal to the number of regions in the atlas. This procedure was done separately for the two cohorts.

Association between cognitive deficits and transcriptomics

For the association between cognitive deficits (CD) and transcriptomics, we first built brain maps of CD using the BrainMap meta-analysis platform (http://www.brainmap.org/). In particular, the Sleuth tool v3.0.3[49] was used to search all the papers in the database using the name of each neuropsychological domain as a keyword. In this way, all the co-activation coordinates that resulted from studies based on functional imaging when the participant in the scanner was performing a task related to each neuropsychological domain were obtained. Next, the GingerAle tool v3.0.2[50] was used to pool all the coordinates onto a single co-activation brain-map for each neuropsychological domain, representing these as a Z-score after applying the activation likelihood estimation (ALE) method. The brain maps were then transformed to the same AAL atlas by calculating the median of all the Z-scores belonging to the same region in the atlas. Finally, the association between CD and transcriptomics was assessed for each gene through the similarity index, equivalent to the Pearson correlation coefficient between CD and transcriptomics, the two variables were represented in the vectors with a dimension equal to the number of regions in the atlas. Transcriptomics correlates were only obtained for those neuropsychological domains that were most affected, identified by choosing a mean Z-score < -2, previously standardized to the normative scores based on a Spanish population. This procedure was done separately for the two cohorts.

DM1 relevant genes and gene ontology

Relevant genes were identified by combining the results from two different strategies. The first was the hypothesis-driven strategy (HDS) that involved reviewing previous studies to identify genes that play a relevant role in some neurobiological aspects of DM1 (Table S2). The second was the data-driven strategy (DDS), which consists of identifying the genes with the strongest transcription correlation with the parameter of interest, either VL or CD. In particular, we chose

bioRxiv preprint doi: https://doi.org/10.1101/2020.07.17.208132; this version posted July 17, 2020. The copyright holder for this preprint (which was not certified by peer review) is the author/funder, who has granted bioRxiv a license to display the preprint in perpetuity. It is made available under aCC-BY-NC-ND 4.0 International license.

those genes with similarity index values where $z < -2$ or $z > 2$, i.e.: outliers of the correlation distribution in both the negative and positive tails. Genes in the positive tail ($z > 2$) were designated as *pos-corr* genes (P), whereas those in the negative tail ($z < -2$) were considered *neg-corr* genes (N). For example, when assessing the VL, the P-genes were systematically expressed more strongly than other genes in the brain regions with more pronounced atrophy, whereas the N-genes were expressed much more weakly than the rest. Although this procedure was performed separately for the two cohorts, the P- and N-genes finally adopted were those present in the two cohorts. We also considered those genes that were expressed similarly to the P- and N-genes as relevant genes, which were dubbed *connector hubs* (C). To identify these, we made use of the "gene-expression connectivity matrix" that represents the similarity in expression between gene pairs obtained from the Pearson pairwise correlations for each entry†. For those genes absent in the groups of P- and N-genes, the strength towards the two P- and N-tails was calculated separately. PC-genes were identified as those genes with a Z-score in connectivity strength towards the P-tail >2 and similarly, NC-genes were identified by having a Z-score in the strength towards the N-tail > 2. For the hypothesis-driven genes given in Table S2 that were defined as P or N genes, their statistical significance was assessed by surrogate-data testing. The BrainSMASH tool[51] was used to build null-distributions by generating 10,000 random maps with the same spatial autocorrelation as that for VL or CD.

Finally, we pooled together all the relevant genes (P-genes, N-genes, PC-genes, NC-genes and the genes that were common to PC and NC) to perform unsupervised K-means clustering with the *Silhouette* strategy to identify the optimal number of clusters. For each cluster, we performed a gene ontology *GO biological process*[52] and *Reactome pathways*[53] overrepresentation test using PANTHER v15.0 (http://pantherdb.org/), with the entire Homo Sapiens genome as the reference

† To calculate the correlations, the values corresponding to the different regions in the atlas were considered as observations.

bioRxiv preprint doi: https://doi.org/10.1101/2020.07.17.208132; this version posted July 17, 2020. The copyright holder for this preprint (which was not certified by peer review) is the author/funder, who has granted bioRxiv a license to display the preprint in perpetuity. It is made available under aCC-BY-NC-ND 4.0 International license.

list and applying a Fisher's Exact test with Bonferroni correction ($p < 0.05$). To make the data more readily interpretable, we only reported ≥2 fold enrichment.

Results

A total of 35 DM1 patients and 60 HCs participated in this study, examined in two different cohorts at two distinct centers. In the first of these, 19 DM1 patients were recruited (9 males) with an average age of 53.3 years (range 42.1 – 69.5 years) and with 16.4 years of education (range 8 – 25 years). With respect to the clinical variables, these patients had an average MIRS score of 2.5 (range 1 – 4) and a mean CTG expansion of 522.8 (range 65 – 1733). These patients were compared with 29 well-matched HCs. In the second cohort, 16 DM1 patients were recruited (7 males), with an average age of 48.8 years (range 36.0 – 61.0 years) and 13.2 years of education (range 6 – 22 years). The mean MIRS score in this cohort was 3.5 (range 2 – 5) and with a CTG expansion size of 827.1 (range 267 – 1833). These patients were compared to 31 well-matched HCs, and all the demographic, clinical and neuropsychological variables collected in the study are detailed in Tables 1 and S1. As explained in the Methods, the two cohorts were considered independently for the imaging analyses, obtaining the corresponding VL brain maps and identifying the list of relevant genes for each cohort separately. Subsequently, the two lists of genes were assessed and only the genes common to the two cohorts were analyzed.

The VL brain maps from each cohort consisted of several widespread cortical and subcortical regions (Figure 1A). There was bilateral subcortical VL in the hippocampus, thalamus, basal ganglia and cerebellum, while cortical VL was evident in multiple regions that included part of the temporal, occipital, parietal cortices, precuneus, pars orbitalis and medial prefrontal cortex (for details see Tables S3 and S4). Importantly, the VL maps for the two cohorts differed more in the cortical regions (Dice index, $D = 0.3$) and they were more similar in the subcortical ones ($D = 0.8$), indicating that subcortical atrophy was more prevalent in DM1 and less variable than cortical atrophy.

bioRxiv preprint doi: https://doi.org/10.1101/2020.07.17.208132; this version posted July 17, 2020. The copyright holder for this preprint (which was not certified by peer review) is the author/funder, who has granted bioRxiv a license to display the preprint in perpetuity. It is made available under aCC-BY-NC-ND 4.0 International license.

The main steps in the pipeline were followed to analyze the transcriptomics through AHBA dataset (Figure 1A), providing brain maps of transcriptional activity for each gene that were spatially-correlated with the brain maps of VL and subsequently, with those of CD. A list of the 27 most relevant hypothesis-driven genes in DM1 was drawn up (Figure 1B, for details on references supporting the selection of each gene see Table S2). Of these 27 preselected genes, 4 genes were discarded based on their SP and DS values (*KL*, *SIX5*, *CLCN1*, *CACNA1S)*. These 4 genes had less than 70% SP (Figure 1B), which implied insufficient transcription signal across all the sampling sites. Therefore, the final list of the most relevant hypothesis-driven genes contained: *DMPK*, *HSPB2*, *INSR*, *CPEB4, ANK2, ARHGEF7, SOS1, PHKA1, MBNL1, KIF13A, APP, MAPT, SNCA, MBNL2, RIPK1, PRNP, TARDBP, MAP3K7, BIN1, DMD, LDB3, TTN* and *CAPN3.* When the pairwise gene-to-gene similarity in transcription was evaluated across the brain for these 23 genes, Silhoutte maximization identified three clusters (in yellow, blue and green in Figure 1B), indicative of functional similarities in the transcription signals among the 23 most-relevant genes.

We next applied a DDS that involved identifying the genes from the entire transcriptome with maximal association in the VL maps, resulting in a total of 370 N-genes and 187 P-genes from the 1st cohort, and 441 N-genes and 161 NP-genes from the 2nd one. The genes common to the two cohorts were those finally used in the analysis, a total of 251 N-genes and 101 P-genes (Figure 2A). Interestingly, two of the genes in the list of the 23 most relevant hypothesis-driven genes also appeared in the list of N-genes, *SNCA* and *DMD*, displaying a similar transcription pattern as the *MAPT* gene (blue cluster in Figure 1B). The spatial-correlation of *SNCA* and *DMD* transcription with the amount of VL in the different brain regions proved to be negative for the two genes and smaller in the two cohorts: < -0.52 for *DMD* and < -0.70 for *SNCA* (Figure 2B and Table S5). In addition to identifying the N- and P-genes, we also searched for the NC- and PC-genes (Figure 3A) that represent *hubs* towards the N and P tails of the expression similarity matrix. We found 452 NC-genes, 396 PC-genes, and 238 genes connecting both N- and P-tails. Remarkably, in the group of PC genes we found *LDB3*, *CAPN3* and *HSPB2* that were in the list

bioRxiv preprint doi: https://doi.org/10.1101/2020.07.17.208132; this version posted July 17, 2020. The copyright holder for this preprint (which was not certified by peer review) is the author/funder, who has granted bioRxiv a license to display the preprint in perpetuity. It is made available under aCC-BY-NC-ND 4.0 International license.

of hypothesis-driven genes, belonging to the same cluster of expression similarity (green cluster, Figure 1B). In addition, the preselected gene *PHKA1* was also common to the groups of NC and PC genes.

Pooling the N, P, NC and PC genes together, along with those common to both the NC and PC categories, we adopted a DDS to achieve unsupervised clustering of the expression similarity matrix, identifying two major clusters after Silhouette maximization (in blue and red in Figure 3B). Importantly, the N and P genes fully segregated into the two differentiated clusters, with all the N-genes belonging to the blue cluster and all the P-genes to the red one, thereby confirming the different functional roles of the groups of genes in the N- and P-tails. These two clusters were used separately for gene enrichment analysis (the list of genes included in each cluster are given in Tables S6 and S7). The search for the *GO biological processes* and *Reactome pathways* confirmed the differentiated roles of these two clusters, with the *neg-corr* genes more related to neuronal and synaptic function, involving key synaptic vesicle events such as recycling, localization, endocytosis and exocytosis but also, the dynamics of serotonin and dopamine neurotransmitter release (Figure 3C). By contrast, the cluster of pos-corr genes was more related to non-neuronal activities, such as interferon signaling, endothelial cell differentiation, angiogenesis, blood transport and cell development.

To assess how the transcriptomics correlated with CD, we focused on the neuropsychological domains in which the composite score reflected strong impairment, satisfying $z < -2$, which was only the case for the attention category (1st cohort $z = -2.5$, 2nd cohort $z = -2.62$: see Table 1 and Figure 4A for the distribution of all the Z-score values from the two cohorts). As indicated in the Methods, the attention composite was obtained by averaging the Z-scores for the following domains: Digit span, STROOP word, STROOP color, Simple RT, election RT, Sequential 1 RT, Sequential 2 RT.

bioRxiv preprint doi: https://doi.org/10.1101/2020.07.17.208132; this version posted July 17, 2020. The copyright holder for this preprint (which was not certified by peer review) is the author/funder, who has granted bioRxiv a license to display the preprint in perpetuity. It is made available under aCC-BY-NC-ND 4.0 International license.

We then obtained brain co-activation maps using "Attention" as a keyword for the search in GingerAle (Figure 4B). As for VL, we calculated the association between the attention co-activation maps and transcriptomics by calculating the spatial Pearson correlation between the two Z-score vectors (one value per brain region in the atlas, see the histogram of all the correlations in Figure 4C). There were a total of 217 N-genes (including *SNCA*), 54 P-genes, 336 NC-genes (including *MAPT* from the list of preselected hypothesis-driven genes), 265 PC-genes, and 156 genes common to both the NC- and PC-gene sets (including *PHKA1)*. Pooling together all classes of genes, we followed a DDS of unsupervised clustering and identified two clusters after Silhoutte maximization (Figure 4C, Tables S8 and S9). Like VL, the two clusters were highly segregated and incorporated all *neg-corr* genes in one cluster, which was enriched in genes related to neuronal and synaptic function (Figure 4D), with all the *pos-corr* genes in the other cluster enriched in non-brain related activities.

Discussion

The AHBA provides information on the transcriptome across the brain in unprecedented detail, covering about 3,702 sampling sites and allowing activity patterns to be built for about 20,500 genes as a specific signature for each anatomic region. To date, its use has shed some light on several fundamental aspects of the brain and their association with the transcriptome, such as myelination[54], hierarchical cortical organization[55], visuomotor integration[33] or large-scale connectivity[31,56,57]. In addition it has provided data regarding pathologies, suggesting novel molecular mechanisms underlying some disorders, such as Autism Spectrum Disorder[58] or functional neurological disorder[59]. It is important to emphasize that our methodology, assessing the relationships between brain images associated with neurodegeneration and the entire transcriptome is complementary to other techniques, such as genome-wide association studies (GWAS)[60], simultaneously addressing genotype–phenotype associations from hundreds of thousands to millions of genetic variants in a data-driven manner. However, it is also important to note that such a vast number of multiple-comparisons requires very large samples to achieve statistical power, which is an important limitation for monogenic disorders like DM1.

bioRxiv preprint doi: https://doi.org/10.1101/2020.07.17.208132; this version posted July 17, 2020. The copyright holder for this preprint (which was not certified by peer review) is the author/funder, who has granted bioRxiv a license to display the preprint in perpetuity. It is made available under aCC-BY-NC-ND 4.0 International license.

Monogenic disorders are paradigmatic disease-models of neurogenetic origin, whereby a mutation in a single gene can cause the disease. However, the alterations causing DM1 appear to propagate to a larger proportion of the gene-to-gene interactome, affecting the function of several other genes. Here, we adopted a novel approach using the AHBA to study the transcriptomic correlates of brain damage and CD in DM1 patients, which to our knowledge has yet to be addressed. Our first finding is related precisely to the mutation located in the untranslated region of the DMPK gene, which triggers the disease and that we found to have the lowest DS (0.19) among the panel of the 23 hypothesis-driven preselected genes. Thus, *DMPK* expression was less reproducible in different brain regions and individuals, and consequently, it was more poorly enriched in terms of brain-related biological processes[47]. By contrast, the *SNCA* gene has the highest DS value (0.84). Our second finding is related to the clusters of spatial similarity among the hypothesis-driven genes in DM1. In particular, we found three clusters, one including the *DMPK* gene together with *LDB3*, *CAPN3* and *HSPB2*, these three latter genes associated with VL in DM1 patients. The second cluster contains several genes with a similar expression to *PHKA1,* which was associated with VL and CD in these patients. Finally, the third cluster contains the genes *SNCA*, *DMD* and *MAPT*, and as we show, this cluster plays the most relevant role in VL and CD in DM1.

A DDS revealed the existence of two tails in the distribution of spatial-similarity between transcription activity and VL or CD. Importantly, the three *SNCA*, *DMD*, *MAPT* genes were present in the negative tail ($z < -2$) of neg-corr genes, indicating that in those brain regions where more VL or CD existed the three genes are systematically transcribed more weakly, and vice versa. Thus, in the regions where the three genes are more strongly expressed, VL or CD was less pronounced. Moreover, this cluster was enriched towards brain-related biological activities, such as synaptic vesicle dynamics (recycling, localization, endocytosis and exocytosis), and serotonin and dopamine neurotransmitter release. By contrast, the pos-corr genes belong to the positive tails ($z > -2$) and they were enriched towards non-brain related functions, mainly

bioRxiv preprint doi: https://doi.org/10.1101/2020.07.17.208132; this version posted July 17, 2020. The copyright holder for this preprint (which was not certified by peer review) is the author/funder, who has granted bioRxiv a license to display the preprint in perpetuity. It is made available under aCC-BY-NC-ND 4.0 International license.

interferon signaling, endothelial cell differentiation, angiogenesis or blood transport, processes known to be affected in DM1[2,61–63].

The DDS also revealed novel relationships between the *MAPT*, *SNCA* and *DMD* genes themselves, providing instructions to produce the proteins tau, alpha-synuclein and dystrophin, respectively. These predictions are consistent with previous studies on DM1 patients, for instance the detection of alpha-synuclein Lewy bodies[27], splicing abnormalities in dystrophin[64,65] and tau-positive degenerative neurites (but not Aβ plaques)[66], and more recently it was suggested the molecular pathways that associate the two *DMPK* and *MAPT* genes[24] may be involved in this condition.

The DDS also revealed new genes implicated in DM1, initially absent from the hypothesis-driven list and enriched in brain-related functions, mainly affecting synaptic vesicles or the dopamine and serotonin pathways (Table S10). From the full list of statistically significant contributions, it is important to note that the findings connecting DM1 with key biological processes in the CNS are in full agreement with previous studies showing synaptic protein dysregulation[67,68], events mediated by *RAB3A* upregulation and *SYN1* hyperphosphorylation in transgenic DM1 mice, and also in transfected cells and post-mortem brains of DM1 patients. Moreover, alterations to synaptic proteins have also been seen to cause behavioral and electrophysiological dysfunction, affecting neurotransmitter signaling, and reducing the dopamine and 5-hydroxyindoleacetic acid (a serotonin metabolite) availability. These data are consistent with our results that DM1 is related to alterations in short-term synaptic plasticity and neurochemical functioning.

In conclusion, we have studied two different cohorts of DM1 patients, each one well-matched to a group HCs, and by employing a DDS that addresses all the hypothesis driven preselected genes for DM1, *DMD*, *SNCA* and *MAPT* were seen to have a major influence on brain damage and CD. Moreover, we found an enrichment of key biological processes in the CNS, such as synaptic

bioRxiv preprint doi: https://doi.org/10.1101/2020.07.17.208132; this version posted July 17, 2020. The copyright holder for this preprint (which was not certified by peer review) is the author/funder, who has granted bioRxiv a license to display the preprint in perpetuity. It is made available under aCC-BY-NC-ND 4.0 International license.

vesicle cycling, recycling and dynamics, and also serotonin and dopamine neurotransmitter signaling. Further studies should clarify whether the interactions between *DMD*, *SNCA* and *MAPT* can be generalized to other degenerative or developmental conditions, or if these are specific to DM1.

Acknowledgments

We wish to thank Prof. Virginia Arechavala for providing us with an updated list of relevant genes in DM1, some of which were considered in our study. J.M.C is funded by Ikerbasque: The Basque Foundation for Science and from the Ministerio de Economia, Industria y Competitividad (Spain) and FEDER (grant DPI2016-79874-R), and from the Department of Economic and Infrastructure Development of the Basque Country (Elkartek Program, KK-2018/00032 and KK-2018/00090). A.L.d.M was founded by the Institute of Health Carlos III co-founded by Fondo Europeo de Desarrollo Regional-FEDER (grant PI17/01841), CIBERNED (grant 609), and La Caixa Foundation (grant HR17-00268). A.S was founded by the Institute of Health Carlos III co-founded by Fondo Europeo de Desarrollo Regional-FEDER (grant PI17/01231), and the Basque Government (grant SAIO08-PE08BF01). A.J.M was partially funded by Euskampus Fundazioa and a predoctoral grant from the Basque Government (PRE_2019_1_0070). G.L was founded by a predoctoral grant from the Basque Government (PRE_2016_1_0187).

bioRxiv preprint doi: https://doi.org/10.1101/2020.07.17.208132; this version posted July 17, 2020. The copyright holder for this preprint (which was not certified by peer review) is the author/funder, who has granted bioRxiv a license to display the preprint in perpetuity. It is made available under aCC-BY-NC-ND 4.0 International license.

Tables

Table 1. Demographic, clinical and neuropsychological variables. Mean values (standard deviations in brackets) of the different variables separated by cohort. The neuropsychological variables coincide with the different composite-scores from the different cognitive domains. All the neuropsychological variables were calculated using normative data from a healthy Spanish population except for the IQ. Because the average score for each domain is equal to zero, values lower than zero indicate that the mean values in those domains are lower than those in the healthy population (the smaller the value, the worse the performance): bold values indicate $p < 0.05$. *For gender differences, the Chi^2 test was used.

	1st Cohort	*2nd Cohort*	*t*	*p*	*Effect Size (Cohen)*
Demographic					
N	19	16			
Age, years	53.30 (8.09)	48.75 (7.72)	1.69	.10	0.57
Males, n(%)	9 (47.37)	7 (43.75)	0.05*	.83	-0.07
Education, years	16.37 (4.87)	13.75 (4.85)	1.59	.12	0.54
Clinical					
N	19	16			
CTG expansion size	522.79 (448.44)	827.13 (433.08)	-2.03	.05	-0.69
MIRS	2.47 (0.96)	3.53 (0.83)	-3.37	**.002**	-1.17
Neuropsychological					
N	18	16			
Visuospatial	-0.35 (1.21)	-1.17 (1.34)	1.86	.07	0.64
Verbal memory	-0.04 (2.33)	-0.74 (1.99)	0.94	.36	0.32
Attention	-2.50 (1.92)	-2.62 (2.14)	0.19	.85	0.06
Executive functioning	-0.91 (2.08)	-1.84 (2.40)	1.21	.23	0.42
Visual memory	-0.34 (0.97)	-1.01 (1.14)	1.83	.08	0.64
Intelligence (IQ)	101.11 (11.51)	91.19 (13.61)	2.3	**.03**	0.79

bioRxiv preprint doi: https://doi.org/10.1101/2020.07.17.208132; this version posted July 17, 2020. The copyright holder for this preprint (which was not certified by peer review) is the author/funder, who has granted bioRxiv a license to display the preprint in perpetuity. It is made available under aCC-BY-NC-ND 4.0 International license.

Figures

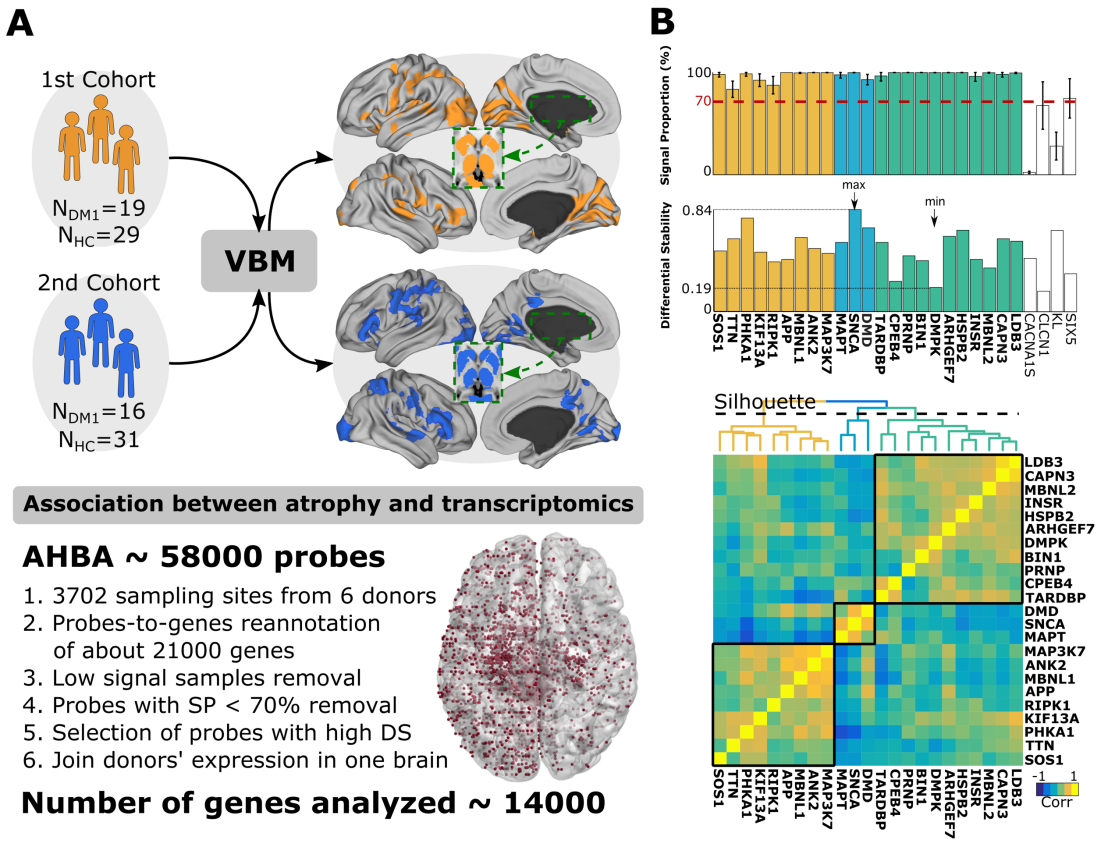

Figure 1. Methodological scheme for the association between transcriptomics and atrophy in DM1, measured as brain volume loss (VL). A: Two cohorts of DM1 patients were recruited (orange and blue) and we obtained the brain maps of the VL for each, comparing the images with a group of HCs using Voxel-Based-Morphometry (VBM), correcting for multiple comparisons. We aimed to characterize the association between VL and transcriptomics, assessing the similarity in the spatial patterns of VL across brain regions and the spatial patterns of gene transcription from the AHBA dataset, preprocessed following a pipeline that is summarized in six main steps (for further details, see methods). After running the AHBA pipeline, about 14K genes finally had transcription values used in the analysis from the 58K probes originally available. The red regions in the brain correspond to the sites at which transcription was sampled. **B:** The sampling proportion (SP) and differential stability (DS) for the 27 preselected hypothesis-driven genes included in the list of candidates relevant to DM1 (obtained by reviewing the literature). The *CACNA1S, CLCN1, KL* and *SIX5* genes did not have a mean SP value above 70% and thus, they were excluded from further analyses. Of the remaining 23 genes, the maximum DS corresponded to *SNCA* and the minimum DS to *DMPK* (see arrows). By examining the spatial similarity in the transcription values, the remaining 23 candidate genes were clustered into three groups. The blue one formed by *DMD*, *SNCA* and *MAPT* played a major role in the characterization of VL. Abbreviations: Muscular Dystrophy Type I (DM1); Healthy Control (HC); Voxel-based morphometry (VBM); Allen Human Brain Atlas (AHBA); Sampling proportion (SP); Differential Stability (DS).

bioRxiv preprint doi: https://doi.org/10.1101/2020.07.17.208132; this version posted July 17, 2020. The copyright holder for this preprint (which was not certified by peer review) is the author/funder, who has granted bioRxiv a license to display the preprint in perpetuity. It is made available under aCC-BY-NC-ND 4.0 International license.

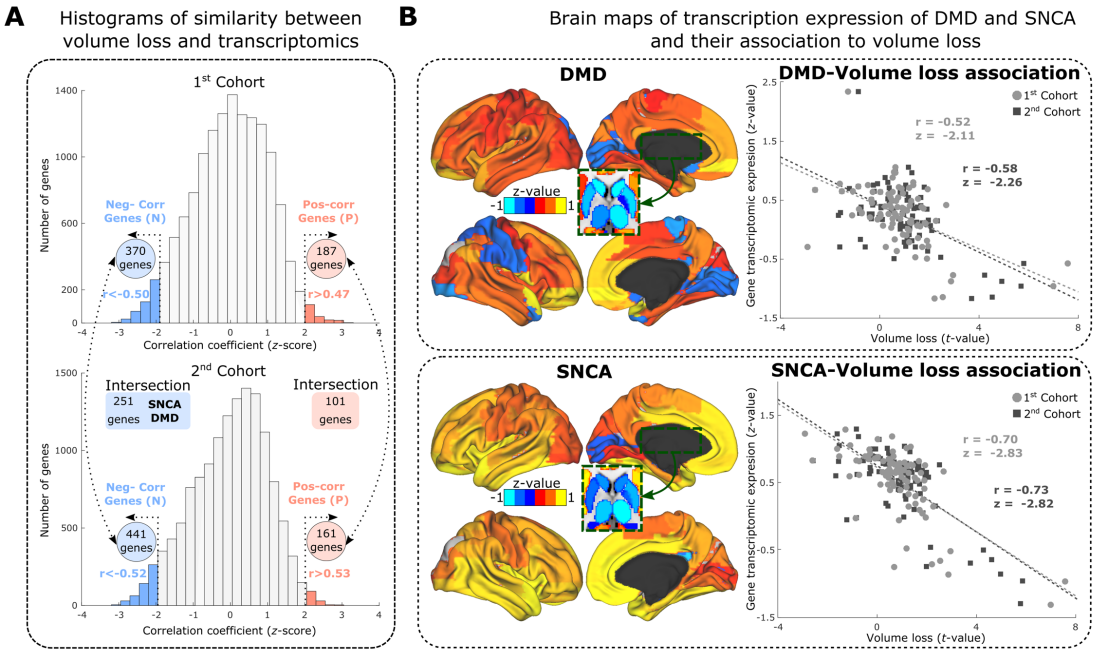

Figure 2. Data-driven strategy to determine the association between the transcriptome and VL in DM1. A: Histogram of the spatial-correlation values (measured as the Z-score) between volume loss (VL) and transcriptional activity for all the genes in both cohorts. For both cohorts the N-genes ($z < -2$) and P-genes ($z > 2$) are colored in blue and red, respectively. The final list of genes used for further analyses are those that are common to the two cohorts, consisting of 251 N-genes and 101 P-genes. From all the genes that provide a maximum association between VL and transcriptomics (Table S6 and S7), only two genes were in the panel of preselected genes: *SNCA* and *DMD*. **B:** Brain maps of transcription in the brain regions for the two genes *DMD* and *SNCA*, which provided a high spatial correlation (r) with the VL brain maps for both cohorts.

bioRxiv preprint doi: https://doi.org/10.1101/2020.07.17.208132; this version posted July 17, 2020. The copyright holder for this preprint (which was not certified by peer review) is the author/funder, who has granted bioRxiv a license to display the preprint in perpetuity. It is made available under aCC-BY-NC-ND 4.0 International license.

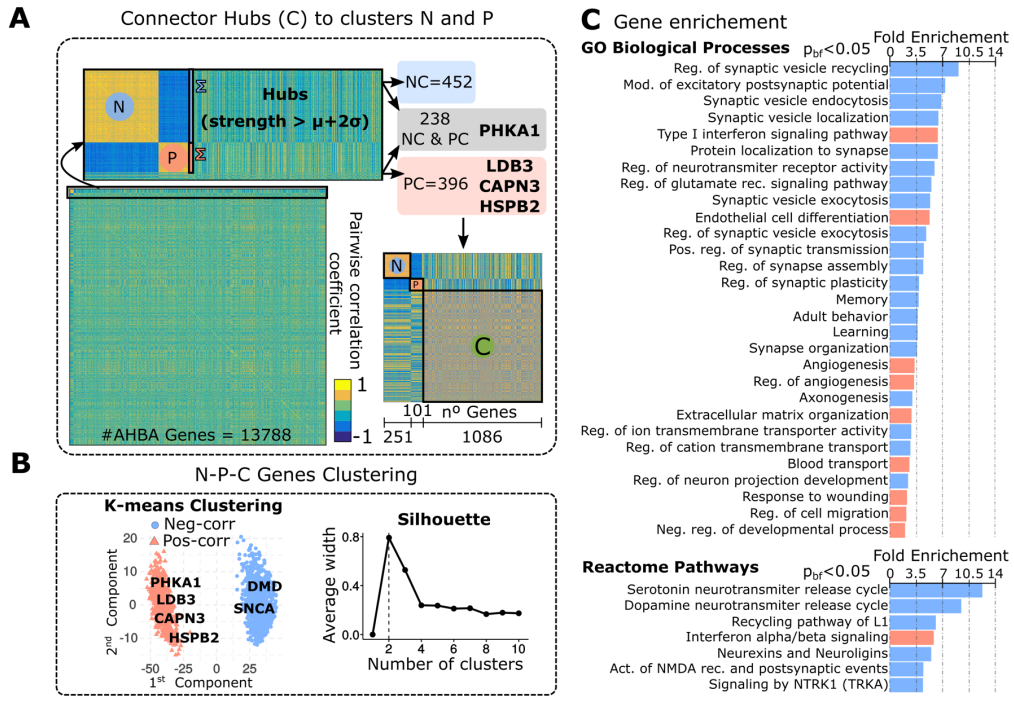

Reg. = Regulation; Mod. = Modulation; Pos. = Positive; Neg. = Negative; CNS = Central Nervous System; Rec. = Receptor/s; Act. = Activation

Figure 3. Functional description of the genes with the highest association with volume loss (VL). A: An all-to-all gene-expression similarity matrix identified the connector hub genes. A total of 1086 genes were found, equal to the sum of the NC = 452 (blue), PC = 396 (red) and 238 common NC and PC genes (gray). **B:** Two clusters were finally found that pooled all gene classes, the blue one contains the original N=251 genes and the red one containing the original P=101 genes. **C:** Gene enrichment for *GO biological process* and *Reactome pathways:* in blue are the neg-corr genes and in red, the pos-corr genes. Abbreviations: Regulation (Reg.); Modulation (Mod.); Positive (Pos.); Negative (Neg.); Central Nervous System (CNS); Receptor/s (Rec.); Activation (Act.).

bioRxiv preprint doi: https://doi.org/10.1101/2020.07.17.208132; this version posted July 17, 2020. The copyright holder for this preprint (which was not certified by peer review) is the author/funder, who has granted bioRxiv a license to display the preprint in perpetuity. It is made available under aCC-BY-NC-ND 4.0 International license.

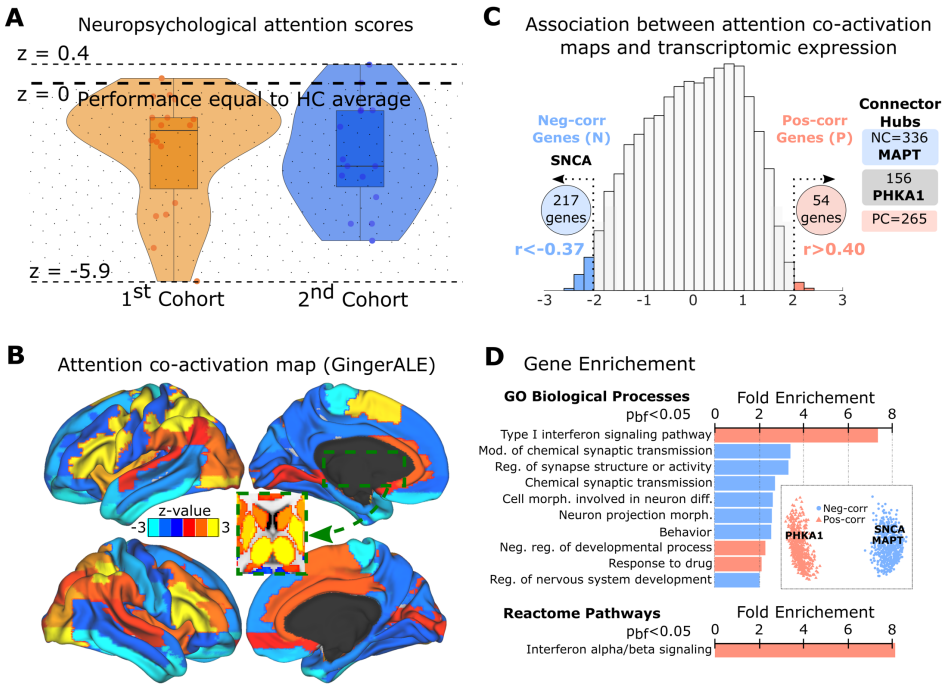

Figure 4. Data-driven strategy to define the association between the transcriptome and attention co-activation maps in DM1. A: Attention scores measured as Z-scores for the two cohorts. Because the Z-scores were normalized to the values in the HCs, negative values of *z* indicate worse performance than the HCs. **B:** Attention co-activation maps built with the GingerALE tool and projected onto the atlas. **C:** Histograms of the spatial correlations between the Z-scores of the attention maps and the transcriptional activity for each gene. The tail of N-genes ($z < -2$, colored in blue) includes the *SNCA* gene from the list of preselected genes, whereas the tail of the P-genes ($z > 2$, red) does not include any of these. Following a procedure similar to that described in Figure 3A, we identified the PC-genes (red), NC-genes (blue, including *MAPT*), and those common to the NC and PC (gray, including *PHKA1*). **D:** After pooling all classes of genes together and clustering, two groups were defined: one including all the neg-corr genes (blue, with *SNCA* and *MAPT)* and one with the pos-corr genes (red, with *PHKA1)*. Gene enrichment for the tags *GO biological process* and *Reactome pathways*. As in Figure 3C, the two clusters also represented two separated functions: the neg-corr one correlated with neuronal functions, whilst the pos-corr correlated to non-brain functions. Abbreviations: Regulation (Reg.); Modulation (Mod.); Positive (Pos.); Negative (Neg.).

bioRxiv preprint doi: https://doi.org/10.1101/2020.07.17.208132; this version posted July 17, 2020. The copyright holder for this preprint (which was not certified by peer review) is the author/funder, who has granted bioRxiv a license to display the preprint in perpetuity. It is made available under aCC-BY-NC-ND 4.0 International license.

References

1. Avaria, M. & Patterson, V. Myotonic dystrophy: relative sensitivity of symptoms signs and abnormal investigations. *Ulster Med. J.* **63**, 151–154 (1994).
2. Lund, M. *et al.* Cardiac involvement in myotonic dystrophy: a nationwide cohort study. *Eur. Heart J.* **35**, 2158–2164 (2014).
3. Bogaard, J. M., van der Meché, F. G., Hendriks, I. & Ververs, C. Pulmonary function and resting breathing pattern in myotonic dystrophy. *Lung* **170**, 143–153 (1992).
4. Ørngreen, M. C., Arlien-Søborg, P., Duno, M., Hertz, J. M. & Vissing, J. Endocrine function in 97 patients with myotonic dystrophy type 1. *J. Neurol.* **259**, 912–920 (2012).
5. Laberge, L., Gagnon, C. & Dauvilliers, Y. Daytime sleepiness and myotonic dystrophy. *Curr. Neurol. Neurosci. Rep.* **13**, 340 (2013).
6. Modoni, A. *et al.* Characterization of the pattern of cognitive impairment in myotonic dystrophy type 1. *Arch. Neurol.* **61**, 1943–1947 (2004).
7. Harper, P. S. *Myotonic dystrophy--the facts: a book for patients and families*. (Oxford University Press, 2002).
8. de Munain, A. L. *et al.* Prevalence of myotonic dystrophy in Guipuzcoa (Basque Country, Spain). *Neurology* **43**, 1573–1573 (1993).
9. Antonini, G. *et al.* Cerebral atrophy in myotonic dystrophy: a voxel based morphometric study. *J. Neurol. Neurosurg. Psychiatry* **75**, 1611–1613 (2004).
10. Weber, Y. G. *et al.* Comparative analysis of brain structure, metabolism, and cognition in myotonic dystrophy 1 and 2. *Neurology* **74**, 1108–1117 (2010).
11. Schneider-Gold, C. *et al.* Cortical and Subcortical Grey and White Matter Atrophy in Myotonic Dystrophies Type 1 and 2 Is Associated with Cognitive Impairment, Depression and Daytime Sleepiness. *PLOS ONE* **10**, e0130352 (2015).
12. Zanigni, S. *et al.* Relationship of white and gray matter abnormalities to clinical and genetic features in myotonic dystrophy type 1. *NeuroImage Clin.* **11**, 678–685 (2016).
13. van Dorst, M. *et al.* Structural white matter networks in myotonic dystrophy type 1. *NeuroImage Clin.* **21**, 101615 (2019).

bioRxiv preprint doi: https://doi.org/10.1101/2020.07.17.208132; this version posted July 17, 2020. The copyright holder for this preprint (which was not certified by peer review) is the author/funder, who has granted bioRxiv a license to display the preprint in perpetuity. It is made available under aCC-BY-NC-ND 4.0 International license.

14. Bertram, L., McQueen, M. B., Mullin, K., Blacker, D. & Tanzi, R. E. Systematic meta-analyses of Alzheimer disease genetic association studies: the AlzGene database. *Nat. Genet.* **39**, 17–23 (2007).

15. Brook, J. D. *et al.* Molecular basis of myotonic dystrophy: Expansion of a trinucleotide (CTG) repeat at the 3′ end of a transcript encoding a protein kinase family member. *Cell* **68**, 799–808 (1992).

16. Lee, J. E. & Cooper, T. A. Pathogenic mechanisms of myotonic dystrophy. *Biochem. Soc. Trans.* **37**, 1281–1286 (2009).

17. Charizanis, K. *et al.* Muscleblind-like 2-Mediated Alternative Splicing in the Developing Brain and Dysregulation in Myotonic Dystrophy. *Neuron* **75**, 437–450 (2012).

18. Lueck, J. D. *et al.* Chloride channelopathy in myotonic dystrophy resulting from loss of posttranscriptional regulation for CLCN1. *Am. J. Physiol.-Cell Physiol.* **292**, C1291–C1297 (2007).

19. Santoro, M. *et al.* Alternative splicing of human insulin receptor gene (INSR) in type I and type II skeletal muscle fibers of patients with myotonic dystrophy type 1 and type 2. *Mol. Cell. Biochem.* **380**, 259–265 (2013).

20. Fugier, C. *et al.* Misregulated alternative splicing of BIN1 is associated with T tubule alterations and muscle weakness in myotonic dystrophy. *Nat. Med.* **17**, 720–725 (2011).

21. Mankodi, A. *et al.* Myotonic dystrophy in transgenic mice expressing an expanded CUG repeat. *Science* **289**, 1769–1773 (2000).

22. Sistiaga, A. *et al.* Cognitive/personality pattern and triplet expansion size in adult myotonic dystrophy type 1 (DM1): CTG repeats, cognition and personality in DM1. *Psychol. Med.* **40**, 487–495 (2010).

23. Winblad, S., Lindberg, C. & Hansen, S. Cognitive deficits and CTG repeat expansion size in classical myotonic dystrophy type 1 (DM1). *Behav. Brain Funct. BBF* **2**, 16 (2006).

bioRxiv preprint doi: https://doi.org/10.1101/2020.07.17.208132; this version posted July 17, 2020. The copyright holder for this preprint (which was not certified by peer review) is the author/funder, who has granted bioRxiv a license to display the preprint in perpetuity. It is made available under aCC-BY-NC-ND 4.0 International license.

24. Carpentier, C. *et al.* Tau exon 2 responsive elements deregulated in myotonic dystrophy type I are proximal to exon 2 and synergistically regulated by MBNL1 and MBNL2. *Biochim. Biophys. Acta* **1842**, 654–664 (2014).

25. Jiang, H., Mankodi, A., Swanson, M. S., Moxley, R. T. & Thornton, C. A. Myotonic dystrophy type 1 is associated with nuclear foci of mutant RNA, sequestration of muscleblind proteins and deregulated alternative splicing in neurons. *Hum. Mol. Genet.* **13**, 3079–3088 (2004).

26. Annic, A. *et al.* Early dopasensitive Parkinsonism related to myotonic dystrophy type 2. *Mov. Disord. Off. J. Mov. Disord. Soc.* **23**, 2100–2101 (2008).

27. Itoh, K. *et al.* Neuropathology does not Correlate with Regional Differences in the Extent of Expansion of CTG Repeats in the Brain with Myotonic Dystrophy Type 1. *Acta Histochem. Cytochem.* **43**, 149–156 (2010).

28. Serra, L. *et al.* How genetics affects the brain to produce higher-level dysfunctions in myotonic dystrophy type 1. *Funct. Neurol.* **30**, 21–31 (2015).

29. Labayru, G. *et al.* Regional brain atrophy in gray and white matter is associated with cognitive impairment in Myotonic Dystrophy type 1. *NeuroImage Clin.* **24**, 102078 (2019).

30. Hawrylycz, M. J. *et al.* An anatomically comprehensive atlas of the adult human brain transcriptome. *Nature* **489**, 391–399 (2012).

31. Diez, I. & Sepulcre, J. Neurogenetic profiles delineate large-scale connectivity dynamics of the human brain. *Nat. Commun.* **9**, 3876 (2018).

32. Sepulcre, J. *et al.* Neurogenetic contributions to amyloid beta and tau spreading in the human cortex. *Nat. Med.* **24**, 1910–1918 (2018).

33. Bueichekú, E. *et al.* Central neurogenetic signatures of the visuomotor integration system. *Proc. Natl. Acad. Sci.* **117**, 6836–6843 (2020).

34. Mathieu, J., Boivin, H., Meunier, D., Gaudreault, M. & Begin, P. Assessment of a disease-specific muscular impairment rating scale in myotonic dystrophy. *Neurology* **56**, 336–340 (2001).

bioRxiv preprint doi: https://doi.org/10.1101/2020.07.17.208132; this version posted July 17, 2020. The copyright holder for this preprint (which was not certified by peer review) is the author/funder, who has granted bioRxiv a license to display the preprint in perpetuity. It is made available under aCC-BY-NC-ND 4.0 International license.

35. Wechsler, D. & Seisdedos Cubero, N. *WAIS-III escala de inteligencia de Wechsler para adultos-III*. (1999).

36. Lezak, M. D., Howieson, D. B., Loring, D. W., Hannay, H. J. & Fischer, J. S. *Neuropsychological assessment, 4th ed.* xiv, 1016 (Oxford University Press, 2004).

37. Casals-Coll, M. *et al.* Estudios normativos españoles en población adulta joven (proyecto NEURONORMA jóvenes): normas para los test de fluencia verbal. *Neurología* **28**, 33–40 (2013).

38. Pena-Casanova, J. *et al.* Spanish Multicenter Normative Studies (NEURONORMA Project): Norms for Verbal Fluency Tests. *Arch. Clin. Neuropsychol.* **24**, 395–411 (2009).

39. Rey, A. *FTest de Copia y Reproducción de una Figura Compleja*. (Tea Ediciones, S.A., 2009).

40. Adams, N. Contributions to Neuropsychological Assessment: A Clinical Manual, 2nd Ed. *Neurology* **45**, 1637–1637 (1995).

41. Douaud, G. *et al.* Anatomically related grey and white matter abnormalities in adolescent-onset schizophrenia. *Brain* **130**, 2375–2386 (2007).

42. De Las Heras, J. *et al.* Brain Circuit Alterations and Cognitive Disability in Late-Onset Cobalamin D Disorder. *J. Clin. Med.* **9**, 990 (2020).

43. Good, C. D. *et al.* A voxel-based morphometric study of ageing in 465 normal adult human brains. *NeuroImage* **14**, 21–36 (2001).

44. Andersson, J. L. R., Jenkinson, M. & Smith, S. Non-linear registration, aka spatial normalisation. FMRIB Technial Report TR07JA2. *Oxf. Cent. Funct. Magn. Reson. Imaging Brain Dep. Clin. Neurol. Oxf. Univ. Oxf. UK* 22 (2007) doi:10.1016/j.neuroimage.2008.10.055.

45. Arnatkevic Iūtė, A., Fulcher, B. D. & Fornito, A. A practical guide to linking brain-wide gene expression and neuroimaging data. *NeuroImage* **189**, 353–367 (2019).

46. Arloth, J., Bader, D. M., Röh, S. & Altmann, A. Re-Annotator: Annotation Pipeline for Microarray Probe Sequences. *PLOS ONE* **10**, e0139516 (2015).

bioRxiv preprint doi: https://doi.org/10.1101/2020.07.17.208132; this version posted July 17, 2020. The copyright holder for this preprint (which was not certified by peer review) is the author/funder, who has granted bioRxiv a license to display the preprint in perpetuity. It is made available under aCC-BY-NC-ND 4.0 International license.

47. Hawrylycz, M. *et al.* Canonical genetic signatures of the adult human brain. *Nat. Neurosci.* **18**, 1832–1844 (2015).

48. Tzourio-Mazoyer, N. *et al.* Automated anatomical labeling of activations in SPM using a macroscopic anatomical parcellation of the MNI MRI single-subject brain. *NeuroImage* **15**, 273–289 (2002).

49. Laird, A. R., Lancaster, J. L. & Fox, P. T. BrainMap: the social evolution of a human brain mapping database. *Neuroinformatics* **3**, 65–78 (2005).

50. Eickhoff, S. B. *et al.* Coordinate-based activation likelihood estimation meta-analysis of neuroimaging data: a random-effects approach based on empirical estimates of spatial uncertainty. *Hum. Brain Mapp.* **30**, 2907–2926 (2009).

51. Burt, J. B., Helmer, M., Shinn, M., Anticevic, A. & Murray, J. D. Generative modeling of brain maps with spatial autocorrelation. *NeuroImage* **220**, 117038 (2020).

52. Ashburner, M. *et al.* Gene ontology: tool for the unification of biology. The Gene Ontology Consortium. *Nat. Genet.* **25**, 25–29 (2000).

53. Fabregat, A. *et al.* Reactome pathway analysis: a high-performance in-memory approach. *BMC Bioinformatics* **18**, 142 (2017).

54. Ritchie, J., Pantazatos, S. P. & French, L. Transcriptomic characterization of MRI contrast with focus on the T1-w/T2-w ratio in the cerebral cortex. *NeuroImage* **174**, 504–517 (2018).

55. Burt, J. B. *et al.* Hierarchy of transcriptomic specialization across human cortex captured by structural neuroimaging topography. *Nat. Neurosci.* **21**, 1251–1259 (2018).

56. Fornito, A., Arnatkevičiūtė, A. & Fulcher, B. D. Bridging the Gap between Connectome and Transcriptome. *Trends Cogn. Sci.* **23**, 34–50 (2019).

57. Romero-Garcia, R. *et al.* Structural covariance networks are coupled to expression of genes enriched in supragranular layers of the human cortex. *NeuroImage* **171**, 256–267 (2018).

bioRxiv preprint doi: https://doi.org/10.1101/2020.07.17.208132; this version posted July 17, 2020. The copyright holder for this preprint (which was not certified by peer review) is the author/funder, who has granted bioRxiv a license to display the preprint in perpetuity. It is made available under aCC-BY-NC-ND 4.0 International license.

58. Romero-Garcia, R., Warrier, V., Bullmore, E. T., Baron-Cohen, S. & Bethlehem, R. A. I. Synaptic and transcriptionally downregulated genes are associated with cortical thickness differences in autism. *Mol. Psychiatry* **24**, 1053–1064 (2019).

59. Diez, I. *et al.* Early-life trauma endophenotypes and brain circuit–gene expression relationships in functional neurological (conversion) disorder. *Mol. Psychiatry* (2020) doi:10.1038/s41380-020-0665-0.

60. Tam, V. *et al.* Benefits and limitations of genome-wide association studies. *Nat. Rev. Genet.* **20**, 467–484 (2019).

61. Fragola, P. V. *et al.* Cardiac involvement in myotonic dystrophy. *Am. J. Cardiol.* **74**, 1070–1072 (1994).

62. Florek, R. C., Triffon, D. W., Mann, D. E., Ringel, S. P. & Reiter, M. J. Electrocardiographic abnormalities in patients with myotonic dystrophy. *West. J. Med.* **153**, 24–27 (1990).

63. Rhodes, J. D. *et al.* Activation of the innate immune response and interferon signalling in myotonic dystrophy type 1 and type 2 cataracts. *Hum. Mol. Genet.* **21**, 852–862 (2012).

64. Nakamori, M. *et al.* Aberrantly spliced -dystrobrevin alters -syntrophin binding in myotonic dystrophy type 1. *Neurology* **70**, 677–685 (2008).

65. Thangarajh, M. *et al.* Relationships between *DMD* mutations and neurodevelopment in dystrophinopathy. *Neurology* 10.1212/WNL.0000000000008363 (2019) doi:10.1212/WNL.0000000000008363.

66. Kiuchi, A., Otsuka, N., Namba, Y., Nakano, I. & Tomonaga, M. Presenile appearance of abundant Alzheimer's neurofibrillary tangles without senile plaques in the brain in myotonic dystrophy. *Acta Neuropathol. (Berl.)* **82**, 1–5 (1991).

67. Hernández-Hernández, O. *et al.* Myotonic dystrophy CTG expansion affects synaptic vesicle proteins, neurotransmission and mouse behaviour. *Brain* **136**, 957–970 (2013).

68. Hernández-Hernández, O. *et al.* Synaptic protein dysregulation in myotonic dystrophy type 1: Disease neuropathogenesis beyond missplicing. *Rare Dis.* **1**, e25553 (2013).

bioRxiv preprint doi: https://doi.org/10.1101/2020.07.17.208132; this version posted July 17, 2020. The copyright holder for this preprint (which was not certified by peer review) is the author/funder, who has granted bioRxiv a license to display the preprint in perpetuity. It is made available under aCC-BY-NC-ND 4.0 International license.

Supplementary Information

Comparison of the two cohorts

When comparing the demographic, clinical and neuropsychological variables between the two cohorts, we found significant differences in MIRS (p=0.002) and IQ (p=0.03), showing respectively higher MIRS and lower IQ in the second cohort as compared to the first. The differences in CTG expansion size and age were almost significant, with effect size equal to -0.69 and 0.56 respectively, indicating a tendency of higher CTG expansion size and lower age in the second cohort as compared to the first. When comparing the neuropsychological scores between cohorts, no significance differences were found in any of the cognitive domains. Notice that, all the domains had a z-score lower than zero, meaning that the patients in the two cohorts had worse performance than the healthy controls. The more affected domain was the attention, that had a z-score lower than -2 in the two cohorts.

Table S1. Age, gender and years of education between DM1 patients and HCs. Mean values of different variables are shown (standard deviations are given in brackets). *For gender differences, the Chi2 test was used.

	DM1	*HC*	*t*	*p*	*Effect Size (Cohen)*
1st Cohort					
N	19	29			
Age, years	53.30 (8.09)	52.17 (8.05)	0.47	.64	0.14
Males, n(%)	9 (47.37)	12 (41.38)	0.17*	.68	-0.12
Education, years	16.37 (4.87)	14.79 (3.36)	1.33	0.19	0.39
2nd Cohort					
N	16	31			
Age, years	48.75 (7.72)	47.55 (7.54)	0.51	.61	0.16
Males, n(%)	7 (43.75)	14 (45.16)	0.01*	.93	-0.03
Education (years)	13.75 (4.85)	-	-	-	-

Table S2. List of relevant genes for the neurobiological aspects of DM1 obtained after reviewing previous studies. Red rows indicate that these genes were not included in the transcriptomics analyses because they had SP < 70%, in at least one of the donors' brain.

HGNC Symbol	*Human Symbol*	*References*
DMPK	DM1 protein kinase	(1–5)

bioRxiv preprint doi: https://doi.org/10.1101/2020.07.17.208132; this version posted July 17, 2020. The copyright holder for this preprint (which was not certified by peer review) is the author/funder, who has granted bioRxiv a license to display the preprint in perpetuity. It is made available under aCC-BY-NC-ND 4.0 International license.

HSPB2	DMPK-Binding Protein	(6)
INSR	Insulin receptor	(7)
CPEB4	Cytoplasmic polyadenylation element binding protein 4	(8)
ANK2	Ankyrin 2	(9)
ARHGEF7	Rho guanine nucleotide exchange factor 7	(10)
SOS1	SOS Ras/Rac guanine nucleotide exchange factor 1	(11)
PHKA1	Phosphorylase kinase regulatory subunit alpha 1	(12)
MBNL1	Muscleblind-like splicing regulator 1	(13, 14)
KIF13A	Kinesin family member 13A	(11, 15)
APP	Amyloid beta precursor protein	(16)
MAPT	Microtubule associated protein tau	(17)
SNCA	Synuclein alpha	(18, 19)
MBNL2	Muscleblind like splicing regulator 2	(20, 21)
RIPK1	Receptor interacting serine/threonine kinase 1	(22)
KL	Klotho	(23, 24)
PRNP	Prion protein	(25)
TARDBP	TAR DNA binding protein	(26, 27)
SIX5	SIX homeobox 5	(28, 29)
MAP3K7	Mitogen-activated protein kinase kinase kinase 7	(30)
BIN1	Bridging integrator 1	(31)
CLCN1	Chloride voltaje-gated channel 1	(32)
DMD	dystrophin	(33–37)
LDB3	LIM domain binding 3	(38)
TTN	Titin or connectin	(39, 40)
CACNA1S	calcium voltage-gated channel subunit alpha1 A	(41)
CAPN3	Calpain 3	(39)

Table S3. Anatomical characterization of atrophied regions in the 1st Cohort. We only represented those regions having more than 50 voxels of overlapping between with the map of volume loss, resulting from the group comparison contrast DM1 < HC.

Area (AAL)	*Peak x (MNI)*	*Peak y (MNI)*	*Peak z (MNI)*	*Peak p*	*Peak t*	*Mean t*	*N Voxels*	*Vol (mm³)*
Occipital_Mid_L	-46	-76	8	<0.001	5.519	2.857	1308	10464
Thalamus_L	-14	-20	12	<0.001	9.382	6.512	1085	8680
Thalamus_R	14	-20	14	<0.001	10.102	7.006	1053	8424
Postcentral_L	-52	-20	14	<0.001	4.604	2.647	1038	8304
Calcarine_L	2	-66	12	<0.001	6.161	3.060	1024	8192
Lingual_R	8	-62	8	<0.001	6.688	3.244	1014	8112
Lingual_L	-22	-90	-14	<0.001	5.346	2.858	907	7256
Temporal_Sup_L	-50	-22	12	<0.001	5.431	2.907	800	6400
Temporal_Mid_L	-50	-72	14	<0.001	4.573	2.559	798	6384
Calcarine_R	6	-64	10	<0.001	6.742	3.577	757	6056
Cerebellum	4	-54	2	<0.001	4.537	2.550	728	5824
Postcentral_R	64	0	20	<0.001	4.184	2.626	716	5728
Temporal_Sup_R	56	-20	12	0.001	3.464	2.582	705	5640
Parietal_Inf_L	-30	-54	50	<0.001	3.711	2.509	596	4768
Precuneus_R	14	-50	12	<0.001	4.436	2.775	586	4688
Putamen_L	-16	12	-2	<0.001	5.809	3.700	576	4608
Putamen_R	18	12	2	<0.001	5.892	3.671	531	4248

bioRxiv preprint doi: https://doi.org/10.1101/2020.07.17.208132; this version posted July 17, 2020. The copyright holder for this preprint (which was not certified by peer review) is the author/funder, who has granted bioRxiv a license to display the preprint in perpetuity. It is made available under aCC-BY-NC-ND 4.0 International license.

Occipital_Inf_L	-20	-92	-12	<0.001	5.070	2.853	492	3936
Frontal_Inf_Tri_R	52	40	4	<0.001	3.748	2.491	487	3896
Caudate_R	18	14	2	<0.001	5.636	3.608	469	3752
Caudate_L	-16	-18	20	<0.001	6.102	3.470	465	3720
Cuneus_L	2	-74	18	<0.001	3.865	2.509	460	3680
Cuneus_R	4	-74	18	<0.001	4.064	2.655	459	3672
Occipital_Sup_L	-16	-78	40	0.001	3.395	2.422	364	2912
Frontal_Inf_Orb_R	44	38	-4	<0.001	3.733	2.530	361	2888
Rolandic_Oper_L	-50	-22	14	<0.001	5.017	2.800	345	2760
Precentral_R	64	2	22	<0.001	4.004	2.602	329	2632
Frontal_Inf_Orb_L	-32	20	-18	<0.001	3.817	2.529	309	2472
Precentral_L	-34	-18	50	<0.001	4.408	2.593	305	2440
Occipital_Sup_R	22	-78	36	<0.001	4.105	2.674	275	2200
Precuneus_L	0	-62	16	<0.001	4.309	2.657	268	2144
Parietal_Sup_L	-28	-54	50	0.001	3.492	2.382	242	1936
Frontal_Mid_R	32	50	2	<0.001	3.544	2.444	235	1880
Hippocampus_L	-20	-30	-4	<0.001	6.352	3.160	222	1776
Rolandic_Oper_R	62	-4	14	<0.001	3.680	2.601	210	1680
Insula_R	28	10	-16	<0.001	3.689	2.592	201	1608
SupraMarginal_R	40	-34	38	<0.001	3.987	2.685	188	1504
Heschl_R	38	-24	14	<0.001	3.817	2.725	169	1352
Amygdala_R	32	0	-18	<0.001	6.812	4.009	154	1232
Insula_L	-26	8	-14	<0.001	5.338	3.102	149	1192
Frontal_Sup_L	-18	2	56	0.003	3.055	2.411	147	1176
Pallidum_R	18	8	0	<0.001	5.022	3.197	145	1160
Heschl_L	-54	-10	8	<0.001	5.106	3.282	142	1136
Occipital_Inf_R	20	-92	-6	<0.001	4.471	2.611	139	1112
Fusiform_L	-22	-46	-12	0.001	3.440	2.592	136	1088
Temporal_Pole_Sup_L	-34	4	-20	<0.001	5.790	3.130	124	992
Frontal_Inf_Tri_L	-48	16	6	0.007	2.789	2.236	122	976
Parietal_Inf_R	40	-40	40	0.005	2.943	2.313	103	824
Hippocampus_R	18	-30	-4	<0.001	7.510	3.762	99	792
SupraMarginal_L	-52	-24	14	<0.001	3.613	2.426	98	784
ParaHippocampal_R	22	6	-20	<0.001	4.637	2.739	91	728
Amygdala_L	-30	2	-18	<0.001	5.688	3.446	86	688
Olfactory_R	22	8	-14	<0.001	5.564	3.582	69	552
ParaHippocampal_L	-18	-36	-4	<0.001	3.650	2.635	58	464
Occipital_Mid_R	32	-70	28	0.010	2.530	2.190	57	456
Frontal_Sup_R	32	64	10	0.010	2.622	2.246	54	432
Frontal_Sup_Orb_L	-24	10	-14	<0.001	5.237	2.960	51	408
Frontal_Mid_Orb_R	48	50	-2	0.004	3.070	2.371	50	400

Table S4. Anatomical characterization of atrophied regions in the 2nd Cohort. We only represented those regions having more than 50 voxels of overlapping between with the map of volume loss, resulting from the group comparison contrast DM1 < HC.

Area (AAL)	*Peak x (MNI)*	*Peak y (MNI)*	*Peak z (MNI)*	*Peak p*	*Peak t*	*Mean t*	*N Voxels*	*Vol (mm³)*
Cerebellum	-10	-82	-34	<0.001	4.895	2.787	6780	54240
Postcentral_L	-56	-4	44	<0.001	4.798	2.867	1455	11640
Thalamus_L	-18	-24	12	<0.001	8.675	5.260	1043	8344
Thalamus_R	18	-24	12	<0.001	8.665	5.241	987	7896

bioRxiv preprint doi: https://doi.org/10.1101/2020.07.17.208132; this version posted July 17, 2020. The copyright holder for this preprint (which was not certified by peer review) is the author/funder, who has granted bioRxiv a license to display the preprint in perpetuity. It is made available under aCC-BY-NC-ND 4.0 International license.

Frontal_Inf_Tri_R	58	38	16	<0.001	4.390	2.610	956	7648
Parietal_Inf_L	-42	-42	42	<0.001	6.180	3.218	950	7600
Lingual_L	-28	-96	-16	<0.001	4.881	2.901	936	7488
Temporal_Sup_R	60	-6	-6	<0.001	3.718	2.522	925	7400
Frontal_Inf_Tri_L	-42	26	0	<0.001	4.444	2.877	907	7256
Putamen_L	-24	16	2	<0.001	8.163	4.912	876	7008
Postcentral_R	50	-12	28	<0.001	5.501	2.924	859	6872
Caudate_L	-14	16	-2	<0.001	6.778	4.377	825	6600
Putamen_R	20	14	2	<0.001	7.007	3.948	775	6200
Lingual_R	20	-94	-12	<0.001	4.435	2.932	774	6192
Occipital_Mid_L	-32	-90	-6	<0.001	5.038	2.761	730	5840
Caudate_R	18	14	2	<0.001	6.908	4.149	710	5680
Parietal_Sup_R	30	-50	60	<0.001	4.699	2.691	604	4832
Precentral_R	46	-12	38	<0.001	5.030	2.940	598	4784
Calcarine_R	24	-98	2	<0.001	4.061	2.851	573	4584
Temporal_Sup_L	-52	-30	22	<0.001	4.036	2.769	547	4376
Precentral_L	-58	-2	42	<0.001	4.614	2.827	542	4336
Calcarine_L	-8	-60	10	<0.001	4.988	2.800	536	4288
Fusiform_L	-30	-74	-14	<0.001	4.472	2.998	511	4088
Occipital_Inf_L	-32	-88	-6	<0.001	5.138	3.100	482	3856
Parietal_Inf_R	38	-50	54	<0.001	3.936	2.709	482	3856
Occipital_Inf_R	32	-92	-2	<0.001	4.685	3.008	469	3752
SupraMarginal_L	-50	-26	24	<0.001	4.972	2.789	416	3328
Frontal_Inf_Oper_R	50	8	16	0.001	3.494	2.458	380	3040
Precuneus_R	14	-50	20	<0.001	3.743	2.478	369	2952
Occipital_Mid_R	32	-96	6	<0.001	4.929	3.360	353	2824
Frontal_Inf_Orb_L	-40	32	-6	<0.001	4.467	3.000	325	2600
Insula_L	-28	16	4	<0.001	4.972	2.615	325	2600
Cingulum_Mid_R	10	-34	34	0.001	3.478	2.573	296	2368
Cingulum_Mid_L	-2	-34	36	<0.001	3.549	2.589	254	2032
Rolandic_Oper_L	-48	-26	22	<0.001	4.179	2.904	218	1744
Precuneus_L	-8	-58	10	<0.001	4.892	2.978	189	1512
SupraMarginal_R	48	-16	28	<0.001	3.573	2.329	183	1464
Frontal_Inf_Orb_R	36	30	-4	<0.001	3.556	2.601	182	1456
Parietal_Sup_L	-40	-42	56	<0.001	4.560	2.778	169	1352
Occipital_Sup_L	-16	-88	28	0.001	3.441	2.530	162	1296
Pallidum_R	20	8	2	<0.001	5.754	3.467	149	1192
Pallidum_L	-18	6	4	<0.001	5.938	3.369	122	976
Occipital_Sup_R	26	-96	10	<0.001	4.176	3.110	120	960
Rolandic_Oper_R	58	2	4	0.003	3.115	2.452	119	952
Insula_R	32	28	-2	<0.001	3.992	2.747	110	880
Angular_R	38	-58	52	<0.001	3.615	2.575	110	880
Cingulum_Post_R	14	-48	20	0.005	2.955	2.294	104	832
Temporal_Mid_R	50	-14	-14	<0.001	3.962	2.802	104	832
Amygdala_R	24	2	-12	<0.001	4.594	2.648	103	824
Cuneus_R	22	-96	10	<0.001	3.552	2.647	99	792
Hippocampus_L	-20	-28	-6	<0.001	4.259	2.914	91	728
Fusiform_R	30	-84	-4	<0.001	4.219	2.408	90	720
Temporal_Mid_L	-58	-32	8	0.004	2.997	2.316	83	664
Frontal_Mid_R	44	32	18	<0.001	3.627	2.527	75	600
Olfactory_L	-24	6	-14	<0.001	3.924	2.741	60	480
Amygdala_L	-18	0	-12	<0.001	3.996	2.716	60	480
Temporal_Pole_Sup_R	58	2	2	0.001	3.326	2.522	56	448
Cingulum_Post_L	-2	-34	32	0.003	3.126	2.499	55	440

bioRxiv preprint doi: https://doi.org/10.1101/2020.07.17.208132; this version posted July 17, 2020. The copyright holder for this preprint (which was not certified by peer review) is the author/funder, who has granted bioRxiv a license to display the preprint in perpetuity. It is made available under aCC-BY-NC-ND 4.0 International license.

Heschl_L	-36	-30	14	0.004	3.079	2.420	54	432
Olfactory_R	6	18	-4	<0.001	4.663	2.860	50	400

Table S5. Statistical significance (p-value) of hypothesis-driven genes using surrogate-data.

	1st Cohort Volume Loss	*2nd Cohort Volume Loss*	*Attention map*
Hypothesis-driven genes			
SNCA	**0**	**0.0003**	**0.0066**
DMD	**0.0055**	**0.0007**	0.1070
PHKA1	**0.0097**	**0.0130**	**0.0271**
LDB3	**0.0049**	**0.0057**	**0.0150**
CAPN3	**0.0022**	**0.0001**	**0.0439**
HSPB2	**0.0330**	**0.0175**	**0.0310**
MAPT	**0.0189**	**0.0175**	**0.0223**

Table S6. Negative-correlated genes (blue-cluster) used for enrichment (Volume Loss). Z-score* represents for N genes the mean Z-score over the two cohorts in the probability distribution of the spatial correlation between gene-transcription activity and volume loss maps; for connector (C) hubs genes it represents the Z-score in the probability distribution of strength values towards the N-genes cluster.

Gene Symbol	*Gene class*	*Z-score**
VXN	N	-3.02
NCAM2	N	-2.93
MEST	N	-2.89
SVOP	N	-2.88
SSTR2	N	-2.87
ENC1	N	-2.86
NPTXR	N	-2.83
SNCA	N	-2.83
CDH9	N	-2.82
GDA	N	-2.81
SLIT1	N	-2.80
PDE1A	N	-2.78
CCN3	N	-2.78
NPTX1	N	-2.77
RASAL1	N	-2.76
RTN4RL2	N	-2.75
TBC1D24	N	-2.71
EFNB2	N	-2.71
FILIP1	N	-2.69
HPCAL4	N	-2.69
SSTR1	N	-2.68
TMEM150C	N	-2.68

bioRxiv preprint doi: https://doi.org/10.1101/2020.07.17.208132; this version posted July 17, 2020. The copyright holder for this preprint (which was not certified by peer review) is the author/funder, who has granted bioRxiv a license to display the preprint in perpetuity. It is made available under aCC-BY-NC-ND 4.0 International license.

CCDC189	N	-2.68
CNIH3	N	-2.68
SHC3	N	-2.67
LINGO1	N	-2.67
NTNG2	N	-2.65
NEURL1B	N	-2.65
STX1A	N	-2.62
KCNG1	N	-2.61
DCAF11	N	-2.60
DACT1	N	-2.60
GPRIN1	N	-2.59
GPM6A	N	-2.59
NFKBIE	N	-2.58
HBQ1	N	-2.58
EMID1	N	-2.57
MIR7-3HG	N	-2.56
CDC42SE2	N	-2.56
MTA3	N	-2.56
BTBD9	N	-2.56
PLXNA1	N	-2.56
ZDHHC23	N	-2.55
ERC2	N	-2.55
ST6GALNAC5	N	-2.55
SYN2	N	-2.54
ARL10	N	-2.54
ASIC2	N	-2.53
DGKZ	N	-2.53
HRK	N	-2.53
CREG2	N	-2.53
DHDH	N	-2.53
FAM131A	N	-2.53
CNRIP1	N	-2.52
MMP16	N	-2.52
MYRIP	N	-2.51
CLSTN2	N	-2.50
KIF21B	N	-2.50
RAET1E-AS1	N	-2.50
NUDT11	N	-2.50
PTPRR	N	-2.49
SHANK1	N	-2.49
KCNMB4	N	-2.48
LAGE3	N	-2.48
RAP1GAP2	N	-2.48
CACNG3	N	-2.47
CXorf49B	N	-2.47
C1orf21	N	-2.47

bioRxiv preprint doi: https://doi.org/10.1101/2020.07.17.208132; this version posted July 17, 2020. The copyright holder for this preprint (which was not certified by peer review) is the author/funder, who has granted bioRxiv a license to display the preprint in perpetuity. It is made available under aCC-BY-NC-ND 4.0 International license.

OGG1	N	-2.47
SEMA4F	N	-2.47
CDH10	N	-2.47
GRIA1	N	-2.46
CENPW	N	-2.45
SLC30A3	N	-2.45
SPINT2	N	-2.45
TCF4	N	-2.45
SCN3B	N	-2.45
LHX6	N	-2.44
CD24	N	-2.44
COG1	N	-2.44
FAM153C	N	-2.44
RMI2	N	-2.44
TSPOAP1	N	-2.44
CNTN1	N	-2.44
RAPH1	N	-2.44
THRB	N	-2.43
STOML1	N	-2.43
SYT17	N	-2.42
FAM19A1	N	-2.42
MTPN	N	-2.42
PRICKLE2	N	-2.41
TYRO3	N	-2.41
SLC39A10	N	-2.41
BEGAIN	N	-2.41
C9orf16	N	-2.41
CALM3	N	-2.41
C2orf80	N	-2.41
SLITRK1	N	-2.41
CHCHD6	N	-2.40
PNCK	N	-2.40
DYNLL1	N	-2.40
MFSD4A	N	-2.40
ARL16	N	-2.39
LMO4	N	-2.38
CEP170B	N	-2.38
DOC2A	N	-2.38
EPHA5	N	-2.38
LMO3	N	-2.38
RILPL2	N	-2.37
SCN9A	N	-2.37
LOC100507387	N	-2.37
PGM2L1	N	-2.36
NAV3	N	-2.36
SLC8A2	N	-2.36

bioRxiv preprint doi: https://doi.org/10.1101/2020.07.17.208132; this version posted July 17, 2020. The copyright holder for this preprint (which was not certified by peer review) is the author/funder, who has granted bioRxiv a license to display the preprint in perpetuity. It is made available under aCC-BY-NC-ND 4.0 International license.

GRIA3	N	-2.36
KCNT2	N	-2.35
MPPED1	N	-2.35
LYRM9	N	-2.35
SNAP25	N	-2.35
FABP3	N	-2.35
PCLO	N	-2.35
ANXA11	N	-2.35
ST3GAL1	N	-2.34
EHBP1L1	N	-2.34
LINC01750	N	-2.34
SPRN	N	-2.34
SLITRK4	N	-2.33
NELL2	N	-2.33
NBEA	N	-2.33
ICAM5	N	-2.33
RAPGEF4	N	-2.33
FAM153A	N	-2.33
TKFC	N	-2.32
HAPLN1	N	-2.32
CSMD1	N	-2.32
NPTX2	N	-2.32
DGKA	N	-2.31
HOPX	N	-2.31
CLEC4G	N	-2.31
PCDH19	N	-2.30
CDK20	N	-2.30
MED10	N	-2.30
DOK6	N	-2.30
RASGRF2	N	-2.30
PLPPR5	N	-2.30
PRKAA2	N	-2.30
CATSPERZ	N	-2.29
SCPEP1	N	-2.29
BAIAP2L2	N	-2.29
RAB15	N	-2.28
VPS37B	N	-2.28
RASL11B	N	-2.28
LRRC28	N	-2.28
CCDC3	N	-2.28
RFTN1	N	-2.28
CCDC71L	N	-2.27
XYLT1	N	-2.27
NOL4	N	-2.27
PRSS3P2	N	-2.27
EFHD2	N	-2.27

bioRxiv preprint doi: https://doi.org/10.1101/2020.07.17.208132; this version posted July 17, 2020. The copyright holder for this preprint (which was not certified by peer review) is the author/funder, who has granted bioRxiv a license to display the preprint in perpetuity. It is made available under aCC-BY-NC-ND 4.0 International license.

FIGNL2	N	-2.27
RAB27B	N	-2.26
LOC728392	N	-2.26
GNB4	N	-2.26
GRK3	N	-2.26
LOC644189	N	-2.25
CAMK2N1	N	-2.25
IQCJ-SCHIP1	N	-2.25
NBL1	N	-2.25
MICAL2	N	-2.24
ENSA	N	-2.24
SLC7A14	N	-2.24
DPF1	N	-2.23
B4GALT5	N	-2.23
RIMBP2	N	-2.23
CALHM2	N	-2.23
MYADM	N	-2.23
GPR22	N	-2.23
FAM102B	N	-2.23
NR4A3	N	-2.23
FHL2	N	-2.23
JPH3	N	-2.23
CCK	N	-2.22
RAP2B	N	-2.22
WNT10B	N	-2.22
SV2B	N	-2.22
SOBP	N	-2.22
ADGRB3	N	-2.21
CRSP8P	N	-2.21
CELF5	N	-2.21
ARMCX2	N	-2.21
FAM81A	N	-2.21
CAMK2A	N	-2.21
GOLGA3	N	-2.21
ARF3	N	-2.21
EXTL1	N	-2.21
PGBD5	N	-2.20
TTC9B	N	-2.20
BEX2	N	-2.20
PPP1R37	N	-2.20
C14orf132	N	-2.20
LRRC8B	N	-2.20
CELF4	N	-2.20
FADS3	N	-2.19
CES4A	N	-2.19
DMD	N	-2.19

bioRxiv preprint doi: https://doi.org/10.1101/2020.07.17.208132; this version posted July 17, 2020. The copyright holder for this preprint (which was not certified by peer review) is the author/funder, who has granted bioRxiv a license to display the preprint in perpetuity. It is made available under aCC-BY-NC-ND 4.0 International license.

HSD11B1L	N	-2.18
TUB	N	-2.18
UBALD1	N	-2.17
RFC5	N	-2.17
VSTM2L	N	-2.16
INKA2	N	-2.16
BLOC1S6	N	-2.16
MNT	N	-2.15
ZNF184	N	-2.15
SREBF2	N	-2.14
LRRC73	N	-2.14
ARPC5L	N	-2.14
GRAMD4	N	-2.14
TGFBR3L	N	-2.13
KAT14	N	-2.13
PHF13	N	-2.12
C1QL3	N	-2.12
CACNG8	N	-2.12
ABI1	N	-2.11
KIAA0513	N	-2.11
TMEM178A	N	-2.11
TMEM70	N	-2.11
CCND2	N	-2.11
AP3S1	N	-2.11
PITPNM2	N	-2.11
CALML3	N	-2.11
MESP1	N	-2.11
ZC3H15	N	-2.11
PID1	N	-2.09
NECTIN3	N	-2.09
UBE2B	N	-2.09
EPB41L4B	N	-2.08
SCN2A	N	-2.08
FNIP2	N	-2.08
PRRG3	N	-2.08
SLC39A4	N	-2.08
NPDC1	N	-2.07
JPH4	N	-2.07
CAP2	N	-2.06
B4GALT2	N	-2.06
MAFG	N	-2.06
APMAP	N	-2.05
RUNDC3A	N	-2.04
SLC25A44	N	-2.03
DZIP3	N	-2.03
TNFAIP8L1	NC & PC	3.34

bioRxiv preprint doi: https://doi.org/10.1101/2020.07.17.208132; this version posted July 17, 2020. The copyright holder for this preprint (which was not certified by peer review) is the author/funder, who has granted bioRxiv a license to display the preprint in perpetuity. It is made available under aCC-BY-NC-ND 4.0 International license.

RNF24	NC	3.33
TRIB3	NC & PC	3.29
HPRT1	NC	3.25
CHD5	NC & PC	3.22
PDZRN4	NC	3.20
TUBA4B	NC & PC	3.20
GDAP1L1	NC	3.19
LOC389906	NC	3.18
XKR4	NC	3.16
HK1	NC	3.14
C1orf216	NC	3.13
SHANK2	NC	3.13
DIRAS2	NC	3.13
KCNH7	NC	3.12
CERS6	NC & PC	3.11
PTPRK	NC	3.09
KIAA1549	NC	3.09
BASP1-AS1	NC	3.09
DNM1	NC	3.09
JAK3	NC	3.08
C1orf115	NC	3.08
UNC13A	NC	3.07
MRTFA	NC	3.06
FXYD6-FXYD2	NC & PC	3.05
DNM1P35	NC	3.05
SYT1	NC & PC	3.04
NICN1	NC	3.04
SLC4A10	NC & PC	3.03
GPR150	NC & PC	3.02
KHDRBS3	NC	3.02
STK32C	NC	3.01
TUBA1B	NC	3.00
WSB2	NC	2.99
FOXRED2	NC	2.98
NAA30	NC	2.98
AP2A2	NC	2.97
SYTL2	NC	2.96
KLC1	NC	2.96
NEGR1	NC & PC	2.96
RAD23B	NC	2.96
NUDT4P2	NC & PC	2.96
GAP43	NC	2.95
PACSIN1	NC	2.95
PHF24	NC	2.95
DLGAP1-AS4	NC	2.94
CORO1A	NC & PC	2.94

bioRxiv preprint doi: https://doi.org/10.1101/2020.07.17.208132; this version posted July 17, 2020. The copyright holder for this preprint (which was not certified by peer review) is the author/funder, who has granted bioRxiv a license to display the preprint in perpetuity. It is made available under aCC-BY-NC-ND 4.0 International license.

DCAF4	NC	2.92
SMIM10L2B	NC	2.92
NANOS3	NC	2.92
ADRA1B	NC	2.92
CHRM3	NC & PC	2.91
FZR1	NC	2.91
OLFM1	NC & PC	2.90
EHD3	NC	2.89
FHOD3	NC	2.89
UNC5A	NC & PC	2.89
SPATS2	NC & PC	2.89
ADCK5	NC	2.88
ARHGDIG	NC	2.88
NUDT4	NC & PC	2.88
CYS1	NC	2.88
ATP6V1G2	NC	2.88
DDX10	NC	2.87
CA10	NC & PC	2.87
NAPB	NC & PC	2.87
MBOAT7	NC & PC	2.86
PCYOX1L	NC	2.86
LOC100505915	NC	2.86
CASC15	NC	2.86
LRRTM4	NC	2.86
GPR162	NC	2.85
B3GALT2	NC & PC	2.85
CSPG4P1Y	NC	2.85
DENND3	NC	2.84
LINC02361	NC & PC	2.84
PRKCE	NC & PC	2.84
TMIE	NC & PC	2.84
PRSS3	NC & PC	2.83
SLITRK5	NC & PC	2.83
AGBL4	NC & PC	2.82
SYP	NC	2.81
TMEM132B	NC	2.81
UNC5D	NC & PC	2.81
ATP6V0CP3	NC	2.81
SERPINF1	NC & PC	2.81
GRIN3A	NC & PC	2.80
MRTFB	NC & PC	2.80
ARMCX5	NC	2.80
PLEKHG5	NC & PC	2.80
SH3GL1	NC	2.79
PAK1	NC	2.79
ACOT4	NC	2.79

bioRxiv preprint doi: https://doi.org/10.1101/2020.07.17.208132; this version posted July 17, 2020. The copyright holder for this preprint (which was not certified by peer review) is the author/funder, who has granted bioRxiv a license to display the preprint in perpetuity. It is made available under aCC-BY-NC-ND 4.0 International license.

GABRA3	NC & PC	2.79
SPRED2	NC	2.79
SKAP2	NC & PC	2.79
GNB1L	NC	2.78
ATP6V0D1	NC	2.78
MYCBP2	NC	2.78
TMEM160	NC	2.77
AP2S1	NC	2.77
TECPR1	NC	2.77
IGSF21	NC & PC	2.77
CMTM4	NC	2.77
CHRNA7	NC	2.77
SMIM10L2A	NC	2.76
MON1A	NC	2.76
AP3B2	NC & PC	2.76
KCNN2	NC & PC	2.76
CLSTN1	NC & PC	2.76
FXYD6	NC & PC	2.76
HMGCR	NC & PC	2.75
KRAS	NC	2.75
RNF2	NC & PC	2.75
ARRB2	NC	2.75
LRFN2	NC & PC	2.74
DENR	NC	2.74
NPM2	NC	2.74
SERPINI1	NC	2.74
BRK1	NC	2.73
JOSD1	NC	2.73
DPP10	NC	2.73
PCMT1	NC	2.73
CSGALNACT1	NC	2.72
EMC3	NC	2.72
SIRPA	NC	2.72
SIDT1	NC & PC	2.72
TMEM198	NC & PC	2.71
OXR1	NC & PC	2.71
BEND5	NC	2.71
CHN1	NC & PC	2.71
MRPL37	NC	2.71
ARNTL2	NC & PC	2.70
NLK	NC	2.70
OSCAR	NC	2.69
COL23A1	NC & PC	2.69
CCDC24	NC & PC	2.68
FBXW7	NC & PC	2.68
GNG2	NC & PC	2.68

bioRxiv preprint doi: https://doi.org/10.1101/2020.07.17.208132; this version posted July 17, 2020. The copyright holder for this preprint (which was not certified by peer review) is the author/funder, who has granted bioRxiv a license to display the preprint in perpetuity. It is made available under aCC-BY-NC-ND 4.0 International license.

VPS41	NC	2.68
KCNMA1	NC & PC	2.67
CDC6	NC & PC	2.67
ZWILCH	NC	2.67
UCHL1	NC	2.67
HTR2A	NC & PC	2.66
POC1A	NC	2.66
KCNK1	NC & PC	2.66
ASXL3	NC & PC	2.66
ABRACL	NC	2.65
NRN1	NC & PC	2.65
RASAL2	NC	2.65
RASA2	NC	2.64
AKIRIN2	NC	2.64
PRPH2	NC & PC	2.64
INCENP	NC	2.64
KIF3A	NC & PC	2.64
CHGB	NC & PC	2.64
FAM49A	NC & PC	2.64
EID2B	NC	2.64
BEX5	NC	2.64
KIF17	NC & PC	2.63
LOC440300	NC	2.63
RFPL1S	NC	2.63
KCNJ6	NC & PC	2.63
TWF2	NC	2.63
FLOT2	NC & PC	2.63
OPCML	NC	2.63
DCBLD1	NC	2.62
ST8SIA5	NC	2.62
MPND	NC	2.62
MAGI1	NC	2.62
VSNL1	NC	2.62
OLFM3	NC	2.62
HMGCS1	NC	2.61
DCAF6	NC	2.61
KIAA1549L	NC & PC	2.61
PNMA6E	NC	2.61
RIMS1	NC	2.61
CLTA	NC	2.61
PRKAR1B	NC	2.60
SLC35F1	NC	2.60
SLC17A7	NC & PC	2.60
SHC2	NC	2.60
ZNRF1	NC	2.60
FRRS1L	NC	2.60

bioRxiv preprint doi: https://doi.org/10.1101/2020.07.17.208132; this version posted July 17, 2020. The copyright holder for this preprint (which was not certified by peer review) is the author/funder, who has granted bioRxiv a license to display the preprint in perpetuity. It is made available under aCC-BY-NC-ND 4.0 International license.

ATP6V0C	NC	2.59
GAST	NC & PC	2.59
CMTM1	NC	2.59
PRKRA-AS1	NC	2.59
MAST3	NC	2.58
RSPO2	NC	2.58
DCP2	NC	2.58
OPTN	NC	2.58
LINC01011	NC	2.58
DSTN	NC	2.58
DGCR9	NC	2.57
CYP26B1	NC	2.57
TBPL1	NC	2.57
GABBR2	NC	2.57
PAK3	NC & PC	2.57
FMN2	NC	2.56
CNTN3	NC & PC	2.56
PRSS1	NC & PC	2.56
ADRA2A	NC	2.56
ABCA3	NC	2.56
TMSB10	NC	2.55
ATP6V1A	NC	2.55
ZNF697	NC & PC	2.55
ACVR2A	NC & PC	2.55
AKT3	NC	2.54
FRMPD2B	NC	2.54
KALRN	NC	2.54
TMEM108	NC	2.54
C16orf45	NC	2.54
ETS2	NC	2.53
MEF2C	NC & PC	2.53
TOLLIP	NC & PC	2.53
USP46	NC	2.53
KIFAP3	NC	2.53
FAM13A	NC & PC	2.53
NRXN2	NC	2.52
STXBP5	NC & PC	2.52
RTN1	NC & PC	2.52
ZFR2	NC	2.52
CHP1	NC	2.52
MSL3P1	NC	2.52
ATP6V1C1	NC & PC	2.52
SAMD12	NC	2.51
TMEM59L	NC & PC	2.51
CAMK1D	NC	2.51
CACNB1	NC	2.51

bioRxiv preprint doi: https://doi.org/10.1101/2020.07.17.208132; this version posted July 17, 2020. The copyright holder for this preprint (which was not certified by peer review) is the author/funder, who has granted bioRxiv a license to display the preprint in perpetuity. It is made available under aCC-BY-NC-ND 4.0 International license.

NAA10	NC	2.51
SYBU	NC	2.51
KCNJ3	NC	2.50
AACS	NC & PC	2.50
DISP2	NC & PC	2.50
FBXL2	NC	2.50
UBE2D3	NC	2.50
DOP1A	NC	2.50
TSPAN5	NC & PC	2.50
TRHDE	NC & PC	2.49
PCDHA13	NC	2.49
HERC1	NC	2.49
FOXK2	NC	2.49
FBXO27	NC	2.49
NELL1	NC	2.49
PPP2R5E	NC	2.48
CDH13	NC	2.48
KCNQ2	NC	2.48
RAB24	NC	2.48
PDF	NC	2.48
FBXW9	NC	2.48
TLN2	NC	2.48
PDE4DIP	NC	2.48
IFNGR2	NC	2.47
TNFRSF14	NC	2.47
ZFP1	NC	2.46
MYO16	NC & PC	2.46
BABAM2	NC	2.46
GTDC1	NC	2.46
LOC100996385	NC	2.46
HOMER2	NC	2.46
ACOT2	NC	2.46
MRTO4	NC	2.46
GRIN2A	NC & PC	2.45
COP1	NC	2.45
DNAJA1	NC	2.45
SLX4	NC	2.45
C17orf51	NC	2.45
MYOM2	NC	2.45
SNAI3-AS1	NC	2.45
STXBP1	NC	2.45
PLXNA2	NC	2.44
COG8	NC	2.44
NOL9	NC	2.44
POLR3A	NC	2.44
DLGAP1	NC & PC	2.44

bioRxiv preprint doi: https://doi.org/10.1101/2020.07.17.208132; this version posted July 17, 2020. The copyright holder for this preprint (which was not certified by peer review) is the author/funder, who has granted bioRxiv a license to display the preprint in perpetuity. It is made available under aCC-BY-NC-ND 4.0 International license.

BICD2	NC	2.43
MLLT11	NC & PC	2.43
HCN1	NC & PC	2.43
TUBB2A	NC & PC	2.43
C11orf80	NC	2.43
SYN1	NC & PC	2.43
FAM19A2	NC & PC	2.43
OSBPL10	NC	2.42
C3orf14	NC	2.42
KNSTRN	NC & PC	2.42
TCTE1	NC	2.42
CTNND2	NC	2.42
VWCE	NC	2.42
SH3GLB2	NC	2.42
TRUB1	NC	2.42
AP3M2	NC	2.42
NMT1	NC	2.42
SPATA7	NC	2.41
AMPH	NC & PC	2.41
CDYL2	NC	2.41
BAIAP3	NC & PC	2.41
CEP72	NC	2.41
LCMT1	NC	2.40
NECAB1	NC	2.40
CHRFAM7A	NC	2.40
CYP4X1	NC	2.40
NMNAT2	NC	2.40
TUBB8P12	NC & PC	2.39
P4HA2	NC	2.39
ZNF541	NC & PC	2.39
DSN1	NC	2.39
PNOC	NC	2.39
MAPK11	NC	2.39
BSN	NC	2.38
UBE3A	NC	2.38
BMS1P14	NC	2.38
YWHAH	NC & PC	2.38
UAP1	NC	2.37
NCALD	NC	2.37
ASS1	NC	2.37
CMAS	NC & PC	2.37
GPRASP1	NC	2.37
CRIM1-DT	NC	2.37
NRCAM	NC	2.37
RAN	NC & PC	2.37
FRMPD4	NC	2.36

bioRxiv preprint doi: https://doi.org/10.1101/2020.07.17.208132; this version posted July 17, 2020. The copyright holder for this preprint (which was not certified by peer review) is the author/funder, who has granted bioRxiv a license to display the preprint in perpetuity. It is made available under aCC-BY-NC-ND 4.0 International license.

PI4KA	NC	2.36
GOLGA7B	NC	2.36
COL24A1	NC & PC	2.36
UBE2K	NC	2.36
AGMAT	NC	2.36
ADAM11	NC & PC	2.36
MBLAC1	NC	2.36
SRRD	NC	2.35
HPCAL1	NC	2.35
PITPNB	NC	2.35
SAE1	NC	2.34
SLC4A1AP	NC	2.34
WDR26	NC	2.34
DPP10-AS1	NC	2.34
SMIM29	NC & PC	2.34
CDK5	NC	2.33
ELAVL4	NC	2.33
SBF1	NC	2.33
PKNOX2	NC	2.33
ABR	NC	2.33
SYT16	NC & PC	2.33
ARL15	NC & PC	2.33
SDK1	NC	2.33
TSPAN14	NC & PC	2.33
CLIP3	NC	2.32
ASNSP1	NC	2.32
CCDC85A	NC	2.32
CABP1	NC	2.32
TSTA3	NC	2.32
RGS6	NC	2.32
CDKL1	NC	2.32
UBE2QL1	NC	2.32
ERC2-IT1	NC	2.32
RARS	NC	2.31
GPR26	NC	2.31
UBE2Q2L	NC	2.31
BICDL1	NC	2.31
XK	NC & PC	2.30
WDR47	NC	2.30
MAPRE3	NC	2.30
CZ1P-ASNS	NC	2.30
NDFIP2	NC & PC	2.30
SH3GL2	NC	2.30
SGSM3	NC	2.29
CBX6	NC	2.29
YTHDF2	NC	2.29

bioRxiv preprint doi: https://doi.org/10.1101/2020.07.17.208132; this version posted July 17, 2020. The copyright holder for this preprint (which was not certified by peer review) is the author/funder, who has granted bioRxiv a license to display the preprint in perpetuity. It is made available under aCC-BY-NC-ND 4.0 International license.

NPAS1	NC	2.29
RAB36	NC & PC	2.29
TMEM130	NC	2.29
SLC9A6	NC	2.28
MAPK8	NC	2.28
PHF14	NC & PC	2.28
CDKN3	NC	2.28
PCDHA10	NC	2.28
BRINP2	NC & PC	2.27
LINGO2	NC	2.27
ASNS	NC	2.27
NUAK1	NC	2.27
SULT4A1	NC	2.27
ATL1	PC	2.27
TUBB4B	NC	2.27
TUBA4A	NC	2.27
EMX1	NC	2.26
TPI1	NC	2.26
MPP2	NC	2.26
VPS29	NC	2.26
RASL10A	NC & PC	2.26
CCNA1	NC & PC	2.26
APBA2	NC	2.26
LZTFL1	NC	2.26
CRIP2	NC	2.26
FAM187A	NC	2.26
SATB1	NC	2.26
PDE4D	NC	2.26
SIRPB1	NC	2.25
IL27RA	NC & PC	2.25
RND1	NC	2.25
TSPYL1	NC	2.25
STRIP1	NC	2.25
EPHA4	NC & PC	2.25
RWDD2A	NC	2.24
PNMA5	NC	2.24
ID2	NC	2.24
PPP1R13B	NC	2.24
LRRC75A	NC	2.24
ACAT2	NC	2.24
MAST1	NC	2.23
PRRT1	NC	2.23
NT5DC3	NC & PC	2.23
ADGRB2	NC & PC	2.23
SEMA6B	NC	2.22
TTC9C	NC	2.22

bioRxiv preprint doi: https://doi.org/10.1101/2020.07.17.208132; this version posted July 17, 2020. The copyright holder for this preprint (which was not certified by peer review) is the author/funder, who has granted bioRxiv a license to display the preprint in perpetuity. It is made available under aCC-BY-NC-ND 4.0 International license.

STYK1	NC & PC	2.22
AK5	NC	2.22
R3HDM1	NC	2.22
NRGN	NC	2.22
SOHLH1	NC	2.22
SUSD6	NC	2.21
DAAM1	NC & PC	2.21
SLC7A4	NC	2.21
VKORC1L1	NC	2.21
HS3ST4	NC	2.21
SOCS7	NC	2.21
C1QL2	NC	2.20
AMN1	NC	2.20
MAP2K4	NC	2.20
COL12A1	NC	2.20
NUDT14	NC	2.20
PKP3	NC	2.19
DIO2	NC	2.19
GNG3	NC	2.19
WIPI2	NC	2.19
PNMA3	NC	2.18
FLRT3	NC & PC	2.18
SCN8A	NC	2.18
DNM1P50	NC	2.17
GNPTAB	NC	2.17
NIP7	NC	2.17
RAB3A	NC	2.17
MAL2	NC & PC	2.17
TRAF3	NC	2.17
ACP1	NC	2.17
KLHL23	NC	2.17
PDE2A	NC	2.17
DNAJC2	NC	2.17
MSL3	NC	2.17
SRRM4	NC	2.16
FDFT1	NC	2.16
LRFN4	NC	2.16
TMEM54	NC	2.16
BAIAP2	NC	2.16
CRMP1	NC	2.16
TNFSF13B	NC	2.16
TSHZ3	NC	2.16
YPEL5	NC	2.15
USP7	NC	2.15
CNN1	NC	2.15
FAM20B	NC	2.15

bioRxiv preprint doi: https://doi.org/10.1101/2020.07.17.208132; this version posted July 17, 2020. The copyright holder for this preprint (which was not certified by peer review) is the author/funder, who has granted bioRxiv a license to display the preprint in perpetuity. It is made available under aCC-BY-NC-ND 4.0 International license.

ATP2B4	NC & PC	2.15
C19orf12	NC	2.15
PNMA2	NC	2.15
CA4	NC	2.15
PPP1R26	NC	2.15
SEPT3	NC	2.15
DZIP1	NC	2.15
ANKRD46	NC	2.15
FAM3C	NC	2.15
PANK2	NC	2.14
CACYBP	NC	2.14
MOCS2	NC	2.14
AP2M1	NC	2.14
PI4KAP2	NC	2.14
LRFN3	NC	2.14
GALNT17	NC	2.13
TASP1	NC	2.13
ANKLE2	NC	2.13
CXorf40A	NC	2.13
KIAA1211L	NC	2.12
CDH18	NC	2.12
TBC1D7	NC	2.12
PAK5	NC	2.12
HPS6	NC	2.12
TMEM8B	NC	2.12
FEM1B	NC	2.12
GABRB3	NC	2.11
RGS4	NC	2.11
MAPK1IP1L	NC	2.11
TPI1P2	NC	2.11
LINC00672	NC	2.11
HIVEP1	NC	2.10
STMN2	NC	2.10
FCRLB	NC	2.10
PRDM8	NC & PC	2.09
NETO1	NC	2.09
SETBP1	NC	2.09
ZNF667	NC	2.08
CHL1	NC	2.08
ADCY2	NC	2.08
RTL6	NC	2.08
RNF175	NC	2.08
PPP1R12A	NC	2.07
DUSP6	NC	2.07
ZFP64	NC	2.07
DNM1L	NC	2.06

bioRxiv preprint doi: https://doi.org/10.1101/2020.07.17.208132; this version posted July 17, 2020. The copyright holder for this preprint (which was not certified by peer review) is the author/funder, who has granted bioRxiv a license to display the preprint in perpetuity. It is made available under aCC-BY-NC-ND 4.0 International license.

STMN1	NC	2.06
CA11	NC	2.05
CUL3	NC	2.05
RHCG	NC	2.05
YWHAB	NC	2.05
CRYM	NC & PC	2.05
EIF3C	NC	2.05
WDR54	NC	2.05
PSMG3-AS1	NC	2.05
ZMIZ1	NC	2.04
NFIB	NC	2.04
SEPT9	NC	2.04
HECTD4	NC	2.04
ITPKA	NC	2.04
SNX10	NC	2.04
BUB1B-PAK6	NC	2.04
PRDM10	NC	2.04
KBTBD11	NC	2.04
MED31	NC	2.03
DLX1	NC	2.03
MATK	NC	2.03
CITED1	NC	2.03
BEX3	NC	2.03
PIK3R1	NC	2.02
PSMB7	NC	2.02
ARHGEF3	NC	2.02
UBA1	NC	2.02
LSM11	NC	2.02
BYSL	NC	2.02
TCERG1L	NC	2.02
ATF7IP2	NC	2.02
BEX1	NC	2.01
SMYD2	NC	2.01
ST6GAL2	NC	2.01
RFX3	NC	2.01
SLC35A2	NC	2.01
PARP8	NC	2.01
RPTOR	NC	2.00
TPRG1L	NC	2.00
PLD3	NC	2.00
PCDH20	PC	2.00
NECTIN1	NC	2.00

Table S7. Positive-correlated genes (red-cluster) used for enrichment (Volume Loss). Z-score* represents for P genes the mean Z-score over the two cohorts in the probability distribution of the spatial correlation between gene-transcription activity and volume loss maps;

bioRxiv preprint doi: https://doi.org/10.1101/2020.07.17.208132; this version posted July 17, 2020. The copyright holder for this preprint (which was not certified by peer review) is the author/funder, who has granted bioRxiv a license to display the preprint in perpetuity. It is made available under aCC-BY-NC-ND 4.0 International license.

for connector (C) hubs genes it represents the Z-score in the probability distribution of strength values towards the P-genes cluster.

Gene Symbol	*Gene class*	*Z-score**
MID2	P	2.85
PCP4	P	2.77
LEF1	P	2.77
NEXN	P	2.76
DENND1B	P	2.75
CRABP1	P	2.74
FAM110A	P	2.74
RGS16	P	2.73
HS3ST5	P	2.71
PRKCH	P	2.67
POMC	P	2.66
TCF7L2	P	2.65
GPR4	P	2.65
SUSD2	P	2.61
SYNE4	P	2.60
THSD4	P	2.60
AR	P	2.59
CFC1B	P	2.58
PLCB4	P	2.58
LRRC49	P	2.49
ADM	P	2.48
TES	P	2.47
TGFBR1	P	2.47
MTAP	P	2.46
TRMT10A	P	2.43
ABTB2	P	2.43
DIPK2B	P	2.42
FAM222A	P	2.41
BHLHE41	P	2.41
GADD45B	P	2.36
PPP1R3B	P	2.36
PEBP4	P	2.34
KCND2	P	2.33
AZGP1	P	2.33
SLC39A8	P	2.32
SOAT1	P	2.31
SV2C	P	2.29
PENK	P	2.29
HMBS	P	2.29
PCAT19	P	2.28
ZIC4	P	2.28

bioRxiv preprint doi: https://doi.org/10.1101/2020.07.17.208132; this version posted July 17, 2020. The copyright holder for this preprint (which was not certified by peer review) is the author/funder, who has granted bioRxiv a license to display the preprint in perpetuity. It is made available under aCC-BY-NC-ND 4.0 International license.

PERP	P	2.28
CKMT2	P	2.28
INTS9	P	2.28
MC1R	P	2.27
MX1	P	2.27
INPP5A	P	2.27
SLC9A5	P	2.27
RASD2	P	2.26
ICK	P	2.26
KIAA1324L	P	2.25
GNRH1	P	2.25
HERPUD1	P	2.25
KCNJ14	P	2.24
PBX3	P	2.23
MCAM	P	2.22
FAM210B	P	2.22
OSBPL2	P	2.21
ELMOD2	P	2.21
CNDP1	P	2.21
TRIM73	P	2.21
TRPT1	P	2.21
ANGPT2	P	2.21
TMEM204	P	2.20
ITM2A	P	2.20
RBMS1	P	2.19
SAMD5	P	2.19
FAM20C	P	2.18
FZD10	P	2.17
SLC16A1	P	2.17
MRPL34	P	2.17
CA12	P	2.16
SLC22A23	P	2.16
ANXA3	P	2.16
SPSB1	P	2.16
PDCD1	P	2.16
TRPC3	P	2.15
KLF2	P	2.15
VWF	P	2.15
ACHE	P	2.14
B3GLCT	P	2.14
PLSCR1	P	2.14
PTPRM	P	2.14
SALL2	P	2.13
INHBA	P	2.12
GPR146	P	2.12
APOLD1	P	2.12

bioRxiv preprint doi: https://doi.org/10.1101/2020.07.17.208132; this version posted July 17, 2020. The copyright holder for this preprint (which was not certified by peer review) is the author/funder, who has granted bioRxiv a license to display the preprint in perpetuity. It is made available under aCC-BY-NC-ND 4.0 International license.

ABCG2	P	2.11
CIT	P	2.11
CNKSR3	P	2.09
GTF2IRD1	P	2.09
CLEC2B	P	2.08
AMPD3	P	2.08
TOB1	P	2.07
ZIC1	P	2.07
MECOM	P	2.07
RORA	P	2.05
NT5DC1	P	2.05
ASIC1	P	2.05
NOSTRIN	P	2.03
TCIRG1	P	2.02
GIMAP7	PC	3.40
HEG1	PC	3.27
EMCN	PC	3.20
ST6GALNAC1	PC	3.19
EBF1	NC & PC	3.18
TNFSF10	PC	3.13
TAP1	PC	3.07
A2M	PC	3.05
BTN2A2	NC & PC	3.05
ITGB1	NC & PC	3.05
CARD6	NC & PC	3.04
RHOQ	NC & PC	3.04
FGR	PC	3.03
ATP10A	PC	3.03
PLAT	NC & PC	3.00
B2M	PC	3.00
FLT1	PC	2.98
INS-IGF2	PC	2.98
TBC1D16	PC	2.97
VEGFC	NC & PC	2.97
GNG11	PC	2.97
BCO2	PC	2.95
ZNF260	PC	2.95
APOL3	PC	2.93
SLCO2B1	PC	2.92
DUSP1	PC	2.92
C19orf33	NC & PC	2.91
TTC39A	NC & PC	2.90
NBEAL1	NC & PC	2.90
HLA-E	PC	2.90
UBIAD1	PC	2.88
EMILIN2	PC	2.87

bioRxiv preprint doi: https://doi.org/10.1101/2020.07.17.208132; this version posted July 17, 2020. The copyright holder for this preprint (which was not certified by peer review) is the author/funder, who has granted bioRxiv a license to display the preprint in perpetuity. It is made available under aCC-BY-NC-ND 4.0 International license.

SRARP	PC	2.86
AK2	PC	2.85
MFAP3L	NC & PC	2.85
ITIH5	PC	2.85
SIK3	NC & PC	2.84
GCOM1	PC	2.83
SCLT1	PC	2.83
TAL2	NC & PC	2.82
UBL3	NC & PC	2.82
LOC105274304	NC & PC	2.82
MOB3B	NC & PC	2.82
SMOC2	NC & PC	2.81
ANXA5	PC	2.81
WWP1	NC & PC	2.81
GATD3A	PC	2.80
SINHCAF	NC & PC	2.79
MINDY1	PC	2.79
TGFBR2	NC & PC	2.79
MYL12A	NC & PC	2.79
PHKA2	NC & PC	2.78
SMAD6	PC	2.78
ZFHX4	NC & PC	2.76
IFITM3	PC	2.76
GMNN	PC	2.76
CAPN2	PC	2.76
CDH6	PC	2.75
MCM3AP-AS1	NC & PC	2.75
DUSP16	PC	2.75
CLMN	PC	2.74
RND2	PC	2.73
CFHR1	PC	2.73
TNS1	PC	2.73
SPATA6	PC	2.72
SNCAIP	NC & PC	2.72
NACC2	PC	2.71
IRF7	PC	2.71
ADCY4	PC	2.70
KCNJ2	NC & PC	2.70
RCL1	NC & PC	2.70
IFI44L	PC	2.70
FAXDC2	PC	2.69
RHOB	NC & PC	2.69
SERPINH1	NC & PC	2.69
VEZF1	PC	2.68
SPP1	PC	2.68
HLA-C	PC	2.68

bioRxiv preprint doi: https://doi.org/10.1101/2020.07.17.208132; this version posted July 17, 2020. The copyright holder for this preprint (which was not certified by peer review) is the author/funder, who has granted bioRxiv a license to display the preprint in perpetuity. It is made available under aCC-BY-NC-ND 4.0 International license.

SLC25A13	PC	2.68
NET1	PC	2.68
ECE2	PC	2.67
QDPR	NC & PC	2.67
SLC12A2	PC	2.66
PPIC	PC	2.66
RELL1	NC & PC	2.64
ST6GALNAC3	PC	2.64
CYTH1	PC	2.64
FER1L4	NC & PC	2.64
ABCB7	PC	2.64
EPB41	NC & PC	2.63
CYYR1	PC	2.63
TBX2-AS1	NC & PC	2.63
AS3MT	PC	2.62
ACVRL1	PC	2.62
GINS3	NC & PC	2.62
MCL1	PC	2.62
IVNS1ABP	PC	2.61
TMEM98	PC	2.61
TUBB6	PC	2.61
KRTCAP2	PC	2.60
XAF1	PC	2.60
MTFR1	PC	2.60
TNFRSF12A	NC & PC	2.60
CAVIN2	NC & PC	2.60
RERGL	PC	2.60
C7orf61	PC	2.59
ANGPTL2	NC & PC	2.59
KCNE5	NC & PC	2.59
LIMS1	PC	2.59
GIMAP1	PC	2.58
DIPK1C	PC	2.58
PEAK1	PC	2.58
ZFHX3	PC	2.58
MPP5	PC	2.58
CCDC39	NC & PC	2.58
TMEM229A	PC	2.58
ADSSL1	PC	2.58
NEAT1	PC	2.57
LINC01105	NC & PC	2.57
TTC12	NC & PC	2.57
LOC100233156	NC & PC	2.57
MVP	PC	2.56
TTLL4	PC	2.56
IGFLR1	PC	2.56

bioRxiv preprint doi: https://doi.org/10.1101/2020.07.17.208132; this version posted July 17, 2020. The copyright holder for this preprint (which was not certified by peer review) is the author/funder, who has granted bioRxiv a license to display the preprint in perpetuity. It is made available under aCC-BY-NC-ND 4.0 International license.

IFI27	PC	2.56
NFKBIA	PC	2.55
NFE2L2	PC	2.55
EFNA2	NC & PC	2.55
COLEC12	PC	2.55
LPIN1	PC	2.55
GNG7	NC & PC	2.55
GPR52	NC	2.55
RBBP9	PC	2.54
LINC00597	NC	2.54
PEPD	PC	2.54
POU3F4	NC & PC	2.54
FKBP2	PC	2.54
GIMAP8	PC	2.54
SRGN	NC & PC	2.53
CFH	PC	2.53
SCARA3	PC	2.52
MYOF	PC	2.51
NXPE3	PC	2.51
CA2	PC	2.51
ID1	PC	2.50
MCM7	PC	2.50
CD34	PC	2.50
IKBKB	PC	2.50
NOC3L	PC	2.50
MPST	PC	2.50
ZNF480	PC	2.50
KDSR	NC & PC	2.50
ELK3	PC	2.50
LOC100507642	NC	2.49
KIAA1958	PC	2.49
CAPN3	PC	2.49
DLC1	PC	2.49
MAP2K3	PC	2.48
SLC12A9	PC	2.48
SLC20A2	NC & PC	2.48
IFITM2	PC	2.48
RELT	NC & PC	2.48
GM2A	PC	2.48
PDE10A	NC & PC	2.47
SLC31A2	PC	2.47
RPS16	PC	2.47
PDE9A	NC & PC	2.46
FOXC1	NC & PC	2.46
OR7E14P	NC & PC	2.46
CAST	PC	2.46

bioRxiv preprint doi: https://doi.org/10.1101/2020.07.17.208132; this version posted July 17, 2020. The copyright holder for this preprint (which was not certified by peer review) is the author/funder, who has granted bioRxiv a license to display the preprint in perpetuity. It is made available under aCC-BY-NC-ND 4.0 International license.

GPER1	PC	2.46
FN1	PC	2.45
SYNE3	PC	2.45
EML4	PC	2.45
DRD2	NC & PC	2.45
C15orf41	NC & PC	2.45
SERPINB1	NC & PC	2.44
GFRA1	PC	2.44
CLEC14A	PC	2.44
WIPI1	PC	2.44
CNTLN	NC & PC	2.44
OSBPL9	PC	2.44
RNF130	PC	2.44
TBL1Y	PC	2.44
SERPINB6	PC	2.44
TIPARP	PC	2.43
OCLN	NC & PC	2.43
LCA5	NC & PC	2.43
FBXO30	PC	2.43
CTPS2	NC & PC	2.43
ACY1	PC	2.43
CCDC80	NC & PC	2.43
MITF	NC & PC	2.42
HLA-G	PC	2.42
MCM5	NC & PC	2.42
ARHGEF10	PC	2.42
LSS	PC	2.42
PMEPA1	PC	2.42
LOC284454	PC	2.42
DISP1	NC & PC	2.42
OR7E156P	PC	2.42
PIM3	PC	2.41
RNF122	PC	2.41
SPOCK3	PC	2.41
CD82	PC	2.41
BBX	PC	2.41
NRN1L	NC & PC	2.41
ABCG1	NC & PC	2.41
RRAD	PC	2.40
PRCP	PC	2.40
SRGAP1	NC & PC	2.40
FOXS1	NC & PC	2.39
CLEC3B	PC	2.39
WDFY3-AS2	PC	2.39
LIFR	PC	2.38
PECAM1	PC	2.38

bioRxiv preprint doi: https://doi.org/10.1101/2020.07.17.208132; this version posted July 17, 2020. The copyright holder for this preprint (which was not certified by peer review) is the author/funder, who has granted bioRxiv a license to display the preprint in perpetuity. It is made available under aCC-BY-NC-ND 4.0 International license.

NUDT12	PC	2.38
SLC12A7	PC	2.38
TMEM79	PC	2.38
ADCY3	NC & PC	2.38
LDLRAD4	PC	2.37
ADORA2A	NC & PC	2.37
GGT5	NC & PC	2.37
RGS9	NC & PC	2.37
GPBP1L1	PC	2.37
NCKAP5	PC	2.37
LIPE	PC	2.36
DLL1	PC	2.36
BBS9	PC	2.36
CARD8	PC	2.36
DPYSL5	PC	2.36
NUDT8	NC & PC	2.36
MARVELD1	NC & PC	2.36
KTN1	PC	2.36
NIFK-AS1	PC	2.35
RSAD2	NC & PC	2.35
JHY	NC	2.35
GABPA	NC & PC	2.35
PARP12	PC	2.35
FOXP1	PC	2.35
HAPLN2	PC	2.35
FOXF1	NC & PC	2.35
PCP4L1	NC	2.34
ZDHHC2	PC	2.34
SRPX	NC & PC	2.34
HLA-DPB1	PC	2.34
RCAN1	PC	2.34
CACNA2D2	PC	2.34
LOC641746	PC	2.34
BSPRY	NC & PC	2.34
SCAF11	PC	2.33
TARSL2	PC	2.33
FMC1	PC	2.33
HIGD1B	PC	2.33
HSPB2	PC	2.33
IFITM1	PC	2.33
RCAN3	PC	2.33
LRRC1	NC & PC	2.33
SPRY3	NC & PC	2.33
BDH2	PC	2.32
SAR1B	NC & PC	2.32
CMC4	PC	2.32

bioRxiv preprint doi: https://doi.org/10.1101/2020.07.17.208132; this version posted July 17, 2020. The copyright holder for this preprint (which was not certified by peer review) is the author/funder, who has granted bioRxiv a license to display the preprint in perpetuity. It is made available under aCC-BY-NC-ND 4.0 International license.

HPSE2	PC	2.32
DMAC2L	PC	2.32
CENPQ	PC	2.32
CPXM2	NC & PC	2.32
CPT1B	PC	2.32
RHBDD1	PC	2.32
LHFPL3	PC	2.31
UACA	PC	2.31
TTC38	PC	2.31
TEP1	PC	2.31
OR7E24	NC & PC	2.30
TMEM189	PC	2.30
IFNAR2	PC	2.30
SRRT	PC	2.30
PIP4K2A	PC	2.30
CHD7	PC	2.30
PLOD3	PC	2.30
MYT1	PC	2.30
DEPTOR	PC	2.29
DUT	PC	2.29
EYA1	NC & PC	2.29
PEG3-AS1	NC	2.29
ANKRD13A	PC	2.29
RFXANK	PC	2.29
PLD1	PC	2.29
LINC00886	NC & PC	2.29
C10orf143	PC	2.29
C1QTNF5	NC & PC	2.29
C6orf47	PC	2.29
TMEM173	PC	2.29
SLC48A1	PC	2.28
RTKN	PC	2.28
VANGL1	NC & PC	2.28
HPDL	NC & PC	2.28
ATG4A	PC	2.27
SMIM10	PC	2.27
KLHL13	NC & PC	2.27
BLOC1S5	PC	2.27
LBR	PC	2.27
ISM1	PC	2.26
LYAR	PC	2.26
HLA-J	PC	2.26
FAM133B	PC	2.26
HEYL	NC & PC	2.26
ACTL6A	PC	2.25
CHADL	PC	2.25

bioRxiv preprint doi: https://doi.org/10.1101/2020.07.17.208132; this version posted July 17, 2020. The copyright holder for this preprint (which was not certified by peer review) is the author/funder, who has granted bioRxiv a license to display the preprint in perpetuity. It is made available under aCC-BY-NC-ND 4.0 International license.

GALNT15	PC	2.25
LDB3	PC	2.25
THBS2	PC	2.25
HBP1	PC	2.25
SIX3	NC	2.25
SVIP	PC	2.24
ZBED3	PC	2.24
NINL	PC	2.24
COL1A2	PC	2.24
GBP4	NC	2.24
CDH23	NC & PC	2.24
AQP5	PC	2.24
KCNH8	PC	2.24
ZNF366	PC	2.24
TTC7A	PC	2.24
SMTN	PC	2.23
DHFR	PC	2.23
FLI1	PC	2.23
NCAPD2	PC	2.23
SPATA13	NC	2.23
HNRNPF	PC	2.23
TNKS	PC	2.22
PTGDS	PC	2.22
DPY19L4	PC	2.22
TMEM87A	PC	2.22
DTNBP1	NC & PC	2.22
RBPMS	NC & PC	2.21
PXN	PC	2.21
VASP	NC & PC	2.21
ARPC1B	PC	2.21
ISG20	NC & PC	2.21
LOC389834	NC	2.21
C8orf44-SGK3	PC	2.21
MYOZ3	PC	2.20
EMP2	PC	2.20
ZBTB1	NC & PC	2.20
PCBD2	PC	2.20
MTMR10	PC	2.20
DECR1	PC	2.20
ARL13B	PC	2.20
MFNG	NC & PC	2.19
CMPK2	NC & PC	2.19
KCNH2	NC & PC	2.19
GPX7	PC	2.19
CCDC96	NC	2.19
CASP4	NC & PC	2.19

bioRxiv preprint doi: https://doi.org/10.1101/2020.07.17.208132; this version posted July 17, 2020. The copyright holder for this preprint (which was not certified by peer review) is the author/funder, who has granted bioRxiv a license to display the preprint in perpetuity. It is made available under aCC-BY-NC-ND 4.0 International license.

EFNA1	PC	2.18
TBL1X	PC	2.18
HMGXB3	PC	2.18
ZFYVE19	PC	2.18
CDK6	PC	2.18
PXK	PC	2.18
CNTN2	PC	2.18
CLIC4	PC	2.18
ZFP36	PC	2.18
METTL8	PC	2.18
IQCH-AS1	PC	2.18
CCNJ	PC	2.18
SOCS6	PC	2.18
TDRD3	PC	2.18
PHKA1	NC & PC	2.18
MPC1	PC	2.18
CXCR4	NC & PC	2.17
GBP3	PC	2.17
RASGRP3	PC	2.17
CDR2L	PC	2.17
FOXL2	PC	2.17
TMCC3	PC	2.17
ST3GAL5	NC & PC	2.16
IQGAP1	PC	2.16
CYB5R2	PC	2.16
PTPRCAP	NC	2.16
KANK4	NC & PC	2.16
ERMP1	PC	2.16
PTPDC1	NC & PC	2.16
SDHC	PC	2.16
FRAT2	PC	2.16
LAYN	PC	2.16
MIA3	PC	2.16
EPAS1	PC	2.16
COL9A3	PC	2.15
PDPN	PC	2.15
ONECUT2	NC	2.15
BCL2L11	PC	2.15
MAP3K3	PC	2.14
AAMDC	PC	2.14
NPC2	PC	2.14
MGARP	NC	2.14
ERG	PC	2.14
BTBD7	PC	2.14
SLC6A13	PC	2.14
RALGAPA2	PC	2.14

bioRxiv preprint doi: https://doi.org/10.1101/2020.07.17.208132; this version posted July 17, 2020. The copyright holder for this preprint (which was not certified by peer review) is the author/funder, who has granted bioRxiv a license to display the preprint in perpetuity. It is made available under aCC-BY-NC-ND 4.0 International license.

PCTP	PC	2.14
DNM2	PC	2.14
ADAM15	PC	2.14
IPW	PC	2.13
HSPB1	PC	2.13
DDIT3	PC	2.13
PAWR	PC	2.13
CNMD	NC	2.13
TWNK	PC	2.13
SLC38A5	PC	2.13
C19orf18	PC	2.13
OMA1	PC	2.13
CCND1	PC	2.12
EPHX2	PC	2.12
HPN	NC & PC	2.12
BTG2	PC	2.12
CYBA	NC	2.12
NDE1	PC	2.12
SPARC	NC & PC	2.12
ZC3H12C	NC & PC	2.12
RHOG	PC	2.12
PPP1R3D	PC	2.12
NTN1	PC	2.12
GPAT2	NC	2.11
ELOVL5	PC	2.11
TMEM38B	PC	2.11
GJC2	PC	2.11
LINC01792	PC	2.11
FAM118A	NC	2.10
SELENOP	PC	2.10
MUSTN1	PC	2.10
NANOG	NC & PC	2.10
TST	PC	2.10
SP110	PC	2.10
TFEB	PC	2.10
PDZD8	PC	2.10
FAM133CP	PC	2.09
CORO7	NC	2.09
BCHE	PC	2.09
CCDC121	PC	2.09
ZFYVE26	PC	2.09
KIAA0586	PC	2.09
DHFR2	PC	2.09
MID1IP1	PC	2.09
ITGA6	PC	2.09
IFIT5	PC	2.09

bioRxiv preprint doi: https://doi.org/10.1101/2020.07.17.208132; this version posted July 17, 2020. The copyright holder for this preprint (which was not certified by peer review) is the author/funder, who has granted bioRxiv a license to display the preprint in perpetuity. It is made available under aCC-BY-NC-ND 4.0 International license.

ICAM2	PC	2.09
IL32	PC	2.09
RGS2	NC	2.09
LPAR1	PC	2.09
SHROOM4	PC	2.08
C11orf96	PC	2.08
HERC2P9	PC	2.08
RIT1	PC	2.08
AIF1L	PC	2.08
BMP6	PC	2.08
CASP7	PC	2.08
RBPJ	PC	2.08
TMEM235	PC	2.08
AP3B1	PC	2.07
NUDT5	PC	2.07
CERS2	PC	2.07
MATN3	PC	2.07
CLN5	PC	2.07
IGFBPL1	NC	2.07
ECI2	PC	2.07
ECHDC2	PC	2.06
CLCN2	PC	2.06
CPT2	PC	2.06
TMEM86B	NC & PC	2.06
NECAP2	PC	2.06
TANC1	PC	2.06
ZNF93	PC	2.06
CDK2AP1	PC	2.06
LOC646626	NC & PC	2.06
SYCE3	PC	2.06
PSKH1	PC	2.06
ATP10D	NC & PC	2.06
RHOU	PC	2.05
APOC1	NC	2.05
USP3	PC	2.05
KLHL20	PC	2.05
NSMCE4A	PC	2.05
TNFAIP2	PC	2.05
PATZ1	PC	2.05
RABEP2	PC	2.05
ENDOD1	PC	2.05
PNP	PC	2.05
MPZL1	PC	2.05
SGK3	PC	2.05
CSRP1	PC	2.05
EHD1	PC	2.04

bioRxiv preprint doi: https://doi.org/10.1101/2020.07.17.208132; this version posted July 17, 2020. The copyright holder for this preprint (which was not certified by peer review) is the author/funder, who has granted bioRxiv a license to display the preprint in perpetuity. It is made available under aCC-BY-NC-ND 4.0 International license.

CYP2J2	PC	2.04
EDN3	PC	2.04
ANAPC16	PC	2.04
ICE2	PC	2.04
ATP6V0E1	PC	2.04
MBD6	NC	2.04
HADHB	PC	2.04
SLC32A1	PC	2.04
ITPKB	PC	2.04
LAMA4	PC	2.04
TMEM99	PC	2.04
PITPNC1	PC	2.04
NKX6-2	PC	2.03
COL9A2	PC	2.03
LAT	PC	2.03
DHRS13	PC	2.03
RHPN1	NC	2.03
ITGA1	PC	2.03
CTTNBP2	PC	2.03
MRRF	PC	2.03
NCSTN	PC	2.03
OTUD7B	PC	2.03
ERBIN	PC	2.02
SHISAL2A	NC	2.02
DOCK1	PC	2.02
CD9	PC	2.02
NKX3-1	NC & PC	2.01
C1orf54	PC	2.01
APH1B	NC	2.01
ACYP2	PC	2.01
MTUS1	PC	2.01
SLC9A9	PC	2.01
TIMP3	PC	2.01
BCAT1	PC	2.01
MTF1	PC	2.01
ZNF396	NC	2.01
MYRF	PC	2.01
KCNJ10	PC	2.01
MEGF10	PC	2.01
RPS27	PC	2.00
MAP6D1	NC	2.00
BTBD17	PC	2.00
HTRA1	PC	2.00
CPQ	PC	2.00
ATF3	PC	2.00

bioRxiv preprint doi: https://doi.org/10.1101/2020.07.17.208132; this version posted July 17, 2020. The copyright holder for this preprint (which was not certified by peer review) is the author/funder, who has granted bioRxiv a license to display the preprint in perpetuity. It is made available under aCC-BY-NC-ND 4.0 International license.

Table S8. Negative-correlated genes (blue-cluster) used for enrichment (Cognitive Disability). Z-score* represents for N genes the Z-score in the probability distribution of the spatial correlation between gene-transcription activity and cognitive disability maps; for connector (C) hubs genes it represents the Z-score in the probability distribution of strength values towards the N-genes cluster.

Gene Symbol	*Gene class*	*Z-score**
LOC644189	N	-2.54
TGFBR3L	N	-2.52
SSTR2	N	-2.50
EFHD2	N	-2.48
CHRM3	N	-2.46
INKA2	N	-2.46
PTPRR	N	-2.42
SLC8A2	N	-2.42
CDK20	N	-2.41
SHANK1	N	-2.40
NBEA	N	-2.39
MEF2C	N	-2.38
MLLT11	N	-2.38
RASL11B	N	-2.37
ACOT4	N	-2.37
OGG1	N	-2.37
STX1A	N	-2.37
SNCA	N	-2.36
RAB24	N	-2.36
GRM8	N	-2.35
FXYD6-FXYD2	N	-2.35
KIAA1217	N	-2.35
FOXRED2	N	-2.34
SLC25A44	N	-2.34
SV2B	N	-2.34
TSHZ3	N	-2.34
ZNF541	N	-2.33
HOPX	N	-2.33
CCL4L2	N	-2.33
GDA	N	-2.33
ADCK5	N	-2.32
ATP6V0C	N	-2.32
NUDT4P2	N	-2.32
CNRIP1	N	-2.32
SPRN	N	-2.31
HS3ST4	N	-2.31
TTC9B	N	-2.31
KHDRBS3	N	-2.30
TSPOAP1	N	-2.29
DLGAP1-AS4	N	-2.29

bioRxiv preprint doi: https://doi.org/10.1101/2020.07.17.208132; this version posted July 17, 2020. The copyright holder for this preprint (which was not certified by peer review) is the author/funder, who has granted bioRxiv a license to display the preprint in perpetuity. It is made available under aCC-BY-NC-ND 4.0 International license.

PRSS1	N	-2.29
HRK	N	-2.29
SYTL2	N	-2.29
CALM3	N	-2.29
XKR4	N	-2.29
PRSS3	N	-2.27
MPPED1	N	-2.26
FXYD6	N	-2.26
CHAF1B	N	-2.26
PI4KA	N	-2.26
FHL2	N	-2.26
GPRIN1	N	-2.25
NUDT9P1	N	-2.25
PRSS3P2	N	-2.24
SLC30A3	N	-2.24
RAB15	N	-2.24
LMO4	N	-2.24
FRMPD4	N	-2.24
COL24A1	N	-2.24
CDH10	N	-2.24
MICAL2	N	-2.23
SLC4A10	N	-2.23
BASP1-AS1	N	-2.23
GPR150	N	-2.22
MMP16	N	-2.22
TCF4	N	-2.22
RND1	N	-2.22
DCAF11	N	-2.22
SOBP	N	-2.21
PLPBP	N	-2.21
HTR2A	N	-2.21
KIF21B	N	-2.21
ID2	N	-2.21
TMEM70	N	-2.21
JPH4	N	-2.21
LRRC73	N	-2.20
IMMP2L	N	-2.20
SETBP1	N	-2.20
LRRC8B	N	-2.20
ARL16	N	-2.19
RFTN1	N	-2.19
JAK3	N	-2.19
SRRM4	N	-2.18
IGSF21	N	-2.18
SLC39A4	N	-2.18
NICN1	N	-2.17

bioRxiv preprint doi: https://doi.org/10.1101/2020.07.17.208132; this version posted July 17, 2020. The copyright holder for this preprint (which was not certified by peer review) is the author/funder, who has granted bioRxiv a license to display the preprint in perpetuity. It is made available under aCC-BY-NC-ND 4.0 International license.

MEST	N	-2.17
DOC2A	N	-2.17
LINC02361	N	-2.17
TYRO3	N	-2.16
NELL1	N	-2.16
JOSD1	N	-2.16
CCK	N	-2.16
DENND3	N	-2.16
CREG2	N	-2.16
LINC01011	N	-2.16
PAK5	N	-2.16
DIRAS2	N	-2.16
CHN1	N	-2.16
FAM131A	N	-2.15
VSNL1	N	-2.15
NELL2	N	-2.15
SYT1	N	-2.15
GPM6A	N	-2.15
RGS4	N	-2.15
MBLAC1	N	-2.15
PGM2L1	N	-2.14
ADRA2A	N	-2.14
CASC15	N	-2.14
PCLO	N	-2.14
PCYOX1L	N	-2.14
CNTN1	N	-2.14
GEMIN2	N	-2.14
TNFSF13B	N	-2.14
ADNP	N	-2.13
UBE2Q2L	N	-2.13
PAK1	N	-2.13
MYRIP	N	-2.13
USP32P1	N	-2.13
ENC1	N	-2.12
PLXNA2	N	-2.12
AACS	N	-2.12
EXTL1	N	-2.12
GNB1L	N	-2.11
CMTM1	N	-2.11
BCL11A	N	-2.11
HK1	N	-2.11
HPS6	N	-2.11
PTPA	N	-2.11
STAMBPL1	N	-2.11
NPTX1	N	-2.11
LOC645202	N	-2.11

bioRxiv preprint doi: https://doi.org/10.1101/2020.07.17.208132; this version posted July 17, 2020. The copyright holder for this preprint (which was not certified by peer review) is the author/funder, who has granted bioRxiv a license to display the preprint in perpetuity. It is made available under aCC-BY-NC-ND 4.0 International license.

THRB	N	-2.10
ANXA11	N	-2.10
MFSD4A	N	-2.10
LINC00937	N	-2.10
NUDT4	N	-2.10
SSBP3	N	-2.09
NLK	N	-2.09
NMT1	N	-2.09
LOC100996385	N	-2.09
NEGR1	N	-2.09
PNOC	N	-2.08
RSPO2	N	-2.08
PACSIN1	N	-2.08
COA7	N	-2.08
DGKA	N	-2.08
MIR7-3HG	N	-2.08
NUAK1	N	-2.08
SVOP	N	-2.08
NUP85	N	-2.08
ADGRB3	N	-2.08
FBXW7	N	-2.08
GRIN2A	N	-2.08
KIAA1549L	N	-2.07
TMEM132A	N	-2.07
MYEF2	N	-2.07
COL23A1	N	-2.07
ABRACL	N	-2.07
EFNB2	N	-2.07
CDKL1	N	-2.06
APBB1	N	-2.06
GPR162	N	-2.06
CLSTN1	N	-2.06
NPM2	N	-2.06
FAM19A1	N	-2.06
ATP6V1C1	N	-2.06
LOC389906	N	-2.06
UNC5A	N	-2.06
SERPINI1	N	-2.06
LRRTM4	N	-2.06
GPRASP1	N	-2.05
PRKAA2	N	-2.05
LOC100507387	N	-2.05
ZNF786	N	-2.05
UNC5D	N	-2.05
PDE1A	N	-2.05
AMPH	N	-2.05

bioRxiv preprint doi: https://doi.org/10.1101/2020.07.17.208132; this version posted July 17, 2020. The copyright holder for this preprint (which was not certified by peer review) is the author/funder, who has granted bioRxiv a license to display the preprint in perpetuity. It is made available under aCC-BY-NC-ND 4.0 International license.

NCAM2	N	-2.04
NFKBIE	N	-2.04
LRFN2	N	-2.04
RTN1	N	-2.04
KLHL8	N	-2.04
KCNT2	N	-2.04
TTYH3	N	-2.04
CAMK2A	N	-2.04
SCN8A	N	-2.04
TOLLIP	N	-2.03
KCNK1	N	-2.03
CALHM2	N	-2.03
CA11	N	-2.03
GID8	N	-2.03
RFPL1S	N	-2.03
HCN1	N	-2.03
KAT14	N	-2.02
C11orf95	N	-2.02
ENSA	N	-2.02
HERC1	N	-2.02
FOXD4	N	-2.02
EMX1	N	-2.02
GRIN3A	N	-2.02
CYS1	N	-2.02
FAM81A	N	-2.02
FAM160A2	N	-2.02
TRIB3	N	-2.02
LRRC28	N	-2.01
WDR26	N	-2.01
GDAP1L1	N	-2.01
LOC440300	N	-2.01
PNMA1	N	-2.01
SLC35F1	N	-2.01
RPH3A	N	-2.00
DCAF4	N	-2.00
CAND2	N	-2.00
CNN1	N	-2.00
ADRA1B	N	-2.00
ARHGDIG	N	-2.00
DNM1	NC	2.92
KCNH7	NC	2.86
CHD5	NC	2.83
MPND	NC	2.82
CSPG4P1Y	NC	2.81
DNM1P35	NC	2.80
SPRED2	NC	2.80

bioRxiv preprint doi: https://doi.org/10.1101/2020.07.17.208132; this version posted July 17, 2020. The copyright holder for this preprint (which was not certified by peer review) is the author/funder, who has granted bioRxiv a license to display the preprint in perpetuity. It is made available under aCC-BY-NC-ND 4.0 International license.

SLITRK5	NC & PC	2.80
LINC00672	NC	2.80
ST3GAL1	NC	2.77
BAIAP2L2	NC & PC	2.73
ASXL3	NC	2.73
C1orf216	NC	2.72
CABP1	NC & PC	2.72
FRMPD2B	NC	2.69
HIVEP1	NC	2.69
TMIE	NC	2.69
NANOS3	NC	2.68
MYOM2	NC	2.68
NR2F1-AS1	NC	2.68
COL12A1	NC	2.68
ARNTL2	NC	2.67
HPRT1	NC	2.67
AP2S1	NC	2.67
PKNOX2	NC & PC	2.67
DPP10-AS1	NC	2.67
BICDL1	NC	2.67
SATB1	NC	2.67
MRTFA	NC	2.66
PNMA6E	NC	2.66
OLFM3	NC	2.65
FMN1	NC	2.65
HSD11B1L	NC	2.64
SPATS2	NC & PC	2.64
ST8SIA5	NC	2.64
ATP6V0CP3	NC	2.64
RAD23B	NC	2.63
PDZRN4	NC	2.63
CEP170B	NC	2.61
ETS2	NC	2.61
RASA2	NC	2.61
EHD3	NC	2.61
KCNJ3	NC	2.61
KLC1	NC	2.60
FLOT2	NC & PC	2.60
PSMD11	NC	2.60
RUNDC3A	NC	2.60
KIFAP3	NC	2.59
EMC3	NC	2.59
ZNF697	NC & PC	2.58
DSN1	NC	2.57
NCALD	NC	2.57
CHRFAM7A	NC	2.56

bioRxiv preprint doi: https://doi.org/10.1101/2020.07.17.208132; this version posted July 17, 2020. The copyright holder for this preprint (which was not certified by peer review) is the author/funder, who has granted bioRxiv a license to display the preprint in perpetuity. It is made available under aCC-BY-NC-ND 4.0 International license.

R3HDM1	NC	2.56
OLFM1	NC & PC	2.56
STMN1	NC	2.55
SHROOM2	NC	2.54
PNMA5	NC & PC	2.54
TUBA1B	NC	2.54
UBE2QL1	NC & PC	2.54
HTR5A	NC & PC	2.54
BEND5	NC & PC	2.54
GABBR2	NC	2.54
SIDT1	NC	2.54
B3GALT2	NC	2.53
PLXNA1	NC	2.53
CDH13	NC	2.53
PDF	NC	2.53
STXBP5	NC & PC	2.53
FLRT3	NC & PC	2.52
TNFAIP8L1	NC & PC	2.51
CTNNAL1	NC	2.51
TMEM160	NC	2.51
LMTK2	NC & PC	2.50
GRK3	NC	2.50
KRAS	NC	2.50
DCBLD1	NC	2.50
TSPAN5	NC & PC	2.50
DCAF6	NC	2.49
KCNMA1	NC & PC	2.49
PSMG3	NC	2.49
RGS6	NC & PC	2.48
RTN4RL2	NC & PC	2.48
TPI1	NC	2.48
CLTA	NC & PC	2.47
KIF3A	NC	2.47
SERPINF1	NC & PC	2.47
C16orf91	NC	2.47
EHBP1L1	NC & PC	2.46
PNMA3	NC	2.46
DDX10	NC	2.46
TPI1P2	NC	2.46
TUBA4B	NC & PC	2.46
LOC100505915	NC	2.45
TENT4A	NC	2.45
NTN4	NC	2.45
TMEM59L	NC	2.45
MAPK8	NC	2.45
SLITRK4	NC & PC	2.45

bioRxiv preprint doi: https://doi.org/10.1101/2020.07.17.208132; this version posted July 17, 2020. The copyright holder for this preprint (which was not certified by peer review) is the author/funder, who has granted bioRxiv a license to display the preprint in perpetuity. It is made available under aCC-BY-NC-ND 4.0 International license.

LZTFL1	NC	2.45
KLHDC3	NC	2.45
SMYD2	NC & PC	2.45
BRINP2	NC	2.45
STRIP1	NC	2.45
MADCAM1	NC	2.44
SAMD12	NC & PC	2.43
AKT3	NC & PC	2.43
HTR1F	NC	2.43
NRN1	NC	2.42
CA10	NC	2.42
TWF2	NC	2.42
SPATA7	NC	2.42
C9orf129	NC & PC	2.41
SHROOM3	NC	2.41
CDH18	NC & PC	2.41
KIF17	NC & PC	2.41
ADCY2	NC	2.41
ELAVL4	NC & PC	2.41
FBXW9	NC	2.40
NPAS1	NC & PC	2.40
SBNO1	NC & PC	2.40
CNIH3	NC	2.40
PRPH2	NC	2.40
CYP26B1	NC	2.40
SOHLH1	NC & PC	2.40
SYP	NC	2.40
ATP6V1A	NC	2.40
SLC39A10	NC	2.39
LINC01963	NC	2.39
DNM1P50	NC & PC	2.38
WAC-AS1	NC	2.38
C1orf115	NC	2.38
GPR26	NC	2.38
OXR1	NC & PC	2.38
CERS6	NC	2.37
FCRLB	NC	2.37
MRTO4	NC	2.37
FARSA	NC	2.37
CUX2	NC	2.37
SGSM3	NC	2.36
MAPK10	NC & PC	2.36
CEP72	NC	2.36
FIBP	NC	2.36
TOMM40L	NC	2.36
PITPNM2	NC	2.36

bioRxiv preprint doi: https://doi.org/10.1101/2020.07.17.208132; this version posted July 17, 2020. The copyright holder for this preprint (which was not certified by peer review) is the author/funder, who has granted bioRxiv a license to display the preprint in perpetuity. It is made available under aCC-BY-NC-ND 4.0 International license.

MAGI1	NC	2.36
GNG3	NC & PC	2.36
TAGLN3	NC	2.35
OSCAR	NC	2.35
RBFOX3	NC & PC	2.35
PRKCE	NC & PC	2.35
LINC01106	NC	2.35
VPS41	NC	2.35
DGCR5	NC	2.34
GSK3B	NC	2.34
DPP10	NC	2.34
SLC4A1AP	NC	2.34
UBL7	NC	2.33
MELTF	NC	2.33
OPN3	NC	2.33
MAFB	NC & PC	2.33
C11orf87	NC & PC	2.33
TUB	NC	2.32
LOC388242	NC	2.32
PKP3	NC	2.32
NIPAL2	NC & PC	2.32
FAM234B	NC & PC	2.32
AP3B2	NC	2.32
TPK1	NC	2.32
CHML	NC	2.31
PRICKLE1	NC	2.31
CDKN3	NC	2.31
TMEM183A	NC	2.31
CCND2	NC	2.30
LRRC4	NC	2.30
OPCML	NC & PC	2.30
KCNJ6	NC & PC	2.30
RASAL2	NC	2.30
CNTNAP5	NC	2.30
FAM3C	NC	2.30
RAI2	NC	2.30
MYO5A	NC	2.30
FAM162B	NC	2.29
FBXL2	NC	2.29
CCDC85A	NC	2.29
MATK	NC & PC	2.29
PPM1L	NC	2.29
GPR22	NC & PC	2.29
CCDC24	NC	2.28
RASGRF2	NC & PC	2.28
NMNAT2	NC	2.28

bioRxiv preprint doi: https://doi.org/10.1101/2020.07.17.208132; this version posted July 17, 2020. The copyright holder for this preprint (which was not certified by peer review) is the author/funder, who has granted bioRxiv a license to display the preprint in perpetuity. It is made available under aCC-BY-NC-ND 4.0 International license.

PKDCC	NC & PC	2.28
SEZ6L2	NC & PC	2.28
DGCR9	NC	2.27
CCDC3	NC & PC	2.27
HECW1	NC	2.27
RFC2	NC	2.27
APBA2	NC	2.27
KCNIP3	NC	2.26
CLOCK	NC	2.26
PLEKHG5	NC	2.26
ADAM11	NC & PC	2.26
SPINT2	NC	2.26
RASD1	NC	2.26
BICDL2	NC	2.25
GOT1	NC	2.25
NPTXR	NC	2.25
GUCA1B	NC & PC	2.25
PPP2R5E	NC	2.24
ISLR	NC	2.24
LINC00473	NC	2.24
ORC4	NC	2.24
NAA10	NC	2.24
ZMIZ1	NC	2.24
GAP43	NC	2.23
PCMT1	NC	2.23
ZBTB16	NC & PC	2.23
PDE4D	NC	2.23
SPATS2L	NC	2.23
CHRNA7	NC	2.23
SAE1	NC	2.23
TMEM132B	NC	2.23
DCTN3	NC	2.23
LINC00294	NC	2.23
MIEF2	NC	2.23
NECTIN3	NC	2.23
TRHDE	NC & PC	2.23
LAGE3	NC	2.23
AGBL4	NC	2.22
PRC1	NC	2.22
GALNT9	NC	2.22
FADS3	NC	2.22
CIDECP1	NC	2.22
OPTN	NC	2.22
FGF12	NC	2.22
PI4KAP2	NC	2.22
BICD2	NC	2.21

bioRxiv preprint doi: https://doi.org/10.1101/2020.07.17.208132; this version posted July 17, 2020. The copyright holder for this preprint (which was not certified by peer review) is the author/funder, who has granted bioRxiv a license to display the preprint in perpetuity. It is made available under aCC-BY-NC-ND 4.0 International license.

CAMK1D	NC & PC	2.21
SLC45A4	NC	2.21
EPHA5	NC	2.20
GAST	NC & PC	2.20
GOLGA7B	NC	2.20
C1orf21	NC	2.20
CENPBD1P1	NC	2.20
ANKRD24	NC	2.19
RNF175	NC	2.19
DDX1	NC	2.19
FAM13A	NC & PC	2.19
NPTX2	NC	2.19
TCERG1L	NC	2.19
TIMM17A	NC	2.19
CBX6	NC	2.19
PPP1R37	NC	2.19
KCNC2	NC	2.19
PFKP	NC	2.19
NAA30	NC	2.19
DCTN2	NC	2.19
NREP	NC	2.19
PCDHA13	NC	2.18
BEAN1	NC	2.18
GPX1	NC	2.18
CSGALNACT1	NC	2.18
ABCC8	NC & PC	2.18
FSD1	NC	2.18
KCNK12	NC	2.18
TTLL12	NC	2.17
EPHB3	NC	2.17
MAPK14	NC	2.17
ABHD8	NC	2.17
MROH1	NC	2.17
NTNG2	NC	2.16
ANKRD46	NC	2.16
HPCAL1	NC	2.16
ZNF25	NC	2.16
PPIP5K1	NC	2.16
PPP2R2D	NC & PC	2.16
MVD	NC	2.15
PIK3R1	NC	2.15
KBTBD11	NC	2.15
LRRC20	NC	2.15
YPEL5	NC	2.15
GFOD2	NC & PC	2.15
CYP4X1	NC	2.15

bioRxiv preprint doi: https://doi.org/10.1101/2020.07.17.208132; this version posted July 17, 2020. The copyright holder for this preprint (which was not certified by peer review) is the author/funder, who has granted bioRxiv a license to display the preprint in perpetuity. It is made available under aCC-BY-NC-ND 4.0 International license.

ZDHHC21	NC	2.14
RHCG	NC	2.14
PTTG3P	NC	2.14
PPP1R26	NC	2.14
LINGO2	NC	2.13
SBF1	NC	2.13
SULT4A1	NC	2.13
C12orf43	NC & PC	2.13
TPST2	NC	2.13
SORL1	NC	2.12
TNFAIP1	NC	2.12
SCAI	NC	2.12
CAPNS1	NC	2.10
NEURL4	NC	2.10
SUSD5	NC	2.10
PTPRT	NC	2.10
STK32C	NC	2.10
LINC01750	NC	2.10
SREBF2	NC	2.09
GRK2	NC	2.09
PLEKHM3	NC	2.09
DSTN	NC	2.09
SARS	NC	2.09
CNTNAP2	NC	2.09
KLHL18	NC	2.09
PREP	NC & PC	2.09
ZFR2	NC	2.09
SYBU	NC	2.09
RAB40C	NC	2.09
GGA3	NC	2.08
MAL2	PC	2.08
TM6SF1	NC	2.08
ABCA3	NC	2.08
SGTB	NC	2.08
TTC9	NC	2.08
POLR3K	NC	2.08
FAXC	NC	2.08
ZNF821	NC	2.07
MYO15A	NC	2.07
TMEM150C	NC	2.07
KIAA1549	NC	2.07
PPFIA4	NC	2.07
YPEL3	NC	2.07
GRK6	NC	2.07
ALAS1	NC	2.07
FMN2	NC	2.06

bioRxiv preprint doi: https://doi.org/10.1101/2020.07.17.208132; this version posted July 17, 2020. The copyright holder for this preprint (which was not certified by peer review) is the author/funder, who has granted bioRxiv a license to display the preprint in perpetuity. It is made available under aCC-BY-NC-ND 4.0 International license.

KHK	NC	2.06
SRCIN1	NC	2.06
MAPT	NC	2.06
ZDHHC23	NC & PC	2.05
LINGO1	NC	2.05
ATP6V0D1	NC	2.05
MAPK11	NC	2.05
TRAF3	NC	2.05
RMI2	NC	2.05
KALRN	NC	2.05
BABAM1	NC	2.05
FIGNL2	NC	2.05
GSTT2B	NC	2.05
CAMK2G	NC	2.05
PIP4P1	NC	2.05
PLXND1	NC	2.05
ZNF48	NC	2.04
ATRNL1	PC	2.04
ARRB2	NC	2.04
TIAM2	NC	2.04
BMS1P14	NC	2.04
PLD3	NC & PC	2.04
FAM217B	NC	2.04
IRS1	NC	2.04
R3HDM2	NC	2.04
FAM19A2	NC	2.04
UAP1	NC	2.03
ADGRL2	NC	2.03
SH3GL1	NC	2.03
WIPI2	NC	2.03
HYAL3	NC	2.03
CIDEC	NC	2.03
NECAB1	NC	2.03
ATP6V1G2	NC	2.03
PPP6R2	NC	2.03
IFITM10	NC	2.03
BLVRA	NC	2.03
SNTB2	NC	2.03
MED10	NC	2.02
SLF1	NC	2.02
IFT57	NC	2.02
PTPRK	NC	2.02
NDUFAF5	NC	2.02
MAST1	NC	2.02
OSBPL10	NC	2.01
MAPK8IP2	NC	2.01

bioRxiv preprint doi: https://doi.org/10.1101/2020.07.17.208132; this version posted July 17, 2020. The copyright holder for this preprint (which was not certified by peer review) is the author/funder, who has granted bioRxiv a license to display the preprint in perpetuity. It is made available under aCC-BY-NC-ND 4.0 International license.

RTL6	NC	2.01
PIH1D1	NC	2.01
CCDC124	NC	2.01
DGKZ	NC	2.01
MSL3P1	NC	2.00
POP7	NC	2.00
PPIA	NC	2.00

Table S9. Positive-correlated genes (red-cluster) used for enrichment (Cognitive Disability). Z-score* represents for P genes the Z-score in the probability distribution of the spatial correlation between gene-transcription activity and cognitive disability maps; for connector (C) hubs genes it represents the Z-score in the probability distribution of strength values towards the P-genes cluster.

Gene Symbol	*Gene class*	*Z-score**
OR7E14P	P	2.41
HVCN1	P	2.34
GIMAP1	P	2.33
KCNE5	P	2.31
PDPN	P	2.30
SLC16A1	P	2.30
GEMIN5	P	2.26
ANGPT2	P	2.25
PCAT19	P	2.24
ASIC1	P	2.23
CLEC2B	P	2.20
SRPX	P	2.19
SPARC	P	2.18
OR7E156P	P	2.17
PDCD1	P	2.14
PBX3	P	2.13
CYYR1	P	2.13
APH1B	P	2.13
CCDC80	P	2.13
HMX1	P	2.13
LMBR1	P	2.11
ISM1	P	2.11
STK26	P	2.11
RSAD2	P	2.11
TMEM114	P	2.11
INHBA	P	2.10
PEBP4	P	2.09
AQP5	P	2.08
IFITM3	P	2.08
MX1	P	2.08
MXRA8	P	2.08

bioRxiv preprint doi: https://doi.org/10.1101/2020.07.17.208132; this version posted July 17, 2020. The copyright holder for this preprint (which was not certified by peer review) is the author/funder, who has granted bioRxiv a license to display the preprint in perpetuity. It is made available under aCC-BY-NC-ND 4.0 International license.

PATZ1	P	2.07
MTA2	P	2.07
TOB1	P	2.06
CILP	P	2.05
SERPINB1	P	2.05
AR	P	2.05
C15orf41	P	2.05
PTPRM	P	2.04
YIPF6	P	2.04
FOXS1	P	2.03
LINC00687	P	2.03
FGD4	P	2.03
SDCBP	P	2.03
FAM201A	P	2.03
DHODH	P	2.02
SLFN11	P	2.02
CPXM2	P	2.02
TMEM38B	P	2.02
OR7E24	P	2.01
PTPRCAP	P	2.01
VAT1	P	2.01
CDKN2A	P	2.00
SASH1	P	2.00
CA12	NC & PC	2.84
KLHL13	NC & PC	2.80
HEYL	NC & PC	2.75
HLA-G	PC	2.70
TAL2	NC & PC	2.69
TIMP3	PC	2.66
LINC00886	NC & PC	2.65
KDSR	PC	2.64
C19orf33	NC & PC	2.63
PARD3	NC & PC	2.60
TIPARP	PC	2.60
HLA-C	PC	2.59
HEY2	PC	2.59
ZNF462	PC	2.59
ST6GALNAC3	PC	2.59
SINHCAF	NC & PC	2.59
IGFBPL1	NC	2.59
PHKA1	NC & PC	2.58
BCHE	PC	2.58
SALL2	NC & PC	2.58
WWTR1	PC	2.57
KIAA1958	PC	2.57
GPR52	NC	2.57

bioRxiv preprint doi: https://doi.org/10.1101/2020.07.17.208132; this version posted July 17, 2020. The copyright holder for this preprint (which was not certified by peer review) is the author/funder, who has granted bioRxiv a license to display the preprint in perpetuity. It is made available under aCC-BY-NC-ND 4.0 International license.

DHRSX	PC	2.56
KRTCAP2	PC	2.56
NCSTN	PC	2.56
EFNA2	NC & PC	2.54
PRKCH	NC & PC	2.54
SPATA13	NC & PC	2.53
NCKAP5	PC	2.52
EYA1	NC & PC	2.51
SULT1C4	PC	2.51
XAF1	PC	2.50
CACNG4	NC & PC	2.50
PPIC	PC	2.50
CECR2	PC	2.49
C1QTNF5	PC	2.49
ZFHX3	PC	2.48
COL1A2	PC	2.48
MRVI1	PC	2.48
GINS3	NC & PC	2.47
PARP14	PC	2.47
LOC100233156	NC & PC	2.47
DRD2	NC & PC	2.47
SIX3	NC & PC	2.46
PNP	PC	2.46
ELK3	PC	2.46
CARD6	NC & PC	2.45
MYOM1	PC	2.45
RAI14	NC & PC	2.45
EPHX2	NC & PC	2.44
GNRH1	NC	2.44
TTC38	PC	2.44
NECAP2	PC	2.44
CHD7	PC	2.44
DIPK1C	NC & PC	2.43
SNCAIP	NC & PC	2.43
ICE2	PC	2.43
ATP10D	NC & PC	2.43
INSYN2	NC & PC	2.43
PDLIM5	PC	2.43
BROX	PC	2.43
LRRN1	NC & PC	2.42
COLEC12	PC	2.42
CHST14	PC	2.42
LHFPL3	PC	2.42
STMP1	PC	2.42
DARS	PC	2.42
ZNF480	PC	2.42

bioRxiv preprint doi: https://doi.org/10.1101/2020.07.17.208132; this version posted July 17, 2020. The copyright holder for this preprint (which was not certified by peer review) is the author/funder, who has granted bioRxiv a license to display the preprint in perpetuity. It is made available under aCC-BY-NC-ND 4.0 International license.

PLEKHA4	PC	2.42
IFI44	NC & PC	2.41
SEC11A	PC	2.41
SERPINH1	NC & PC	2.41
ZHX2	PC	2.41
BAG3	NC & PC	2.40
TRPS1	PC	2.40
ZFHX4	NC & PC	2.40
CXCR4	NC & PC	2.40
ANKIB1	PC	2.40
PAFAH2	PC	2.39
VASP	NC & PC	2.39
ZIC4	NC & PC	2.39
FAM111A	PC	2.39
RP2	PC	2.38
NBEAL1	NC & PC	2.38
CD38	NC & PC	2.38
CCZ1P-OR7E38P	PC	2.37
ADM	NC & PC	2.37
AP3B1	PC	2.37
RGS9	NC	2.37
TCIRG1	NC & PC	2.37
TENT5A	NC & PC	2.36
BBS9	PC	2.36
CYBA	NC & PC	2.36
IGF2BP2	NC & PC	2.36
EEF1A1	PC	2.36
IRF2	PC	2.35
ABCA1	NC & PC	2.35
H2AFJ	NC & PC	2.35
LRP10	PC	2.35
BNIP2	NC & PC	2.35
SLC40A1	PC	2.35
C11orf71	PC	2.35
SEPT2	PC	2.34
MAP3K1	PC	2.34
ADORA2A	NC	2.34
HSDL2	PC	2.34
ITPKB	PC	2.33
FOXO1	NC & PC	2.33
MORC4	PC	2.33
ITGA1	PC	2.33
SRGAP1	NC & PC	2.33
CDK6	PC	2.32
ACTL6A	PC	2.32
GIMAP7	PC	2.32

bioRxiv preprint doi: https://doi.org/10.1101/2020.07.17.208132; this version posted July 17, 2020. The copyright holder for this preprint (which was not certified by peer review) is the author/funder, who has granted bioRxiv a license to display the preprint in perpetuity. It is made available under aCC-BY-NC-ND 4.0 International license.

CAPN2	PC	2.32
GBP3	NC & PC	2.32
TMEM189	PC	2.32
LINC01105	NC & PC	2.32
EBF1	NC & PC	2.32
SAMD9L	PC	2.31
APOC1	NC & PC	2.31
A2M	PC	2.31
ZFP36L2	PC	2.31
WWP1	NC & PC	2.31
SLCO2B1	PC	2.31
ZNF610	PC	2.31
PINLYP	NC & PC	2.31
ZSWIM6	NC & PC	2.31
ABCG2	PC	2.31
YBX3P1	NC & PC	2.31
COL25A1	NC	2.31
COCH	NC	2.30
EPS8	PC	2.30
FUBP3	PC	2.30
IL13RA1	PC	2.30
THBS2	PC	2.30
WASF2	PC	2.30
OR7E12P	PC	2.30
BTN2A2	NC & PC	2.29
SLC14A1	PC	2.29
FN1	PC	2.29
FAM114A1	PC	2.29
TCF3	PC	2.29
LIFR	PC	2.28
NUP37	NC & PC	2.28
CAMKMT	NC & PC	2.28
ANKRD45	NC	2.28
FAM118A	NC	2.28
NPL	PC	2.28
TMEM167B	PC	2.27
ZC3H12C	NC & PC	2.27
UEVLD	PC	2.27
CMTR2	NC & PC	2.27
CMTM3	PC	2.27
SYCE3	PC	2.27
GNG7	NC & PC	2.27
LIMK2	NC & PC	2.27
C19orf18	PC	2.26
RASL11A	NC & PC	2.26
SZRD1	NC & PC	2.26

bioRxiv preprint doi: https://doi.org/10.1101/2020.07.17.208132; this version posted July 17, 2020. The copyright holder for this preprint (which was not certified by peer review) is the author/funder, who has granted bioRxiv a license to display the preprint in perpetuity. It is made available under aCC-BY-NC-ND 4.0 International license.

PELI2	PC	2.26
HLA-E	PC	2.26
RBMS3	PC	2.25
CNMD	NC	2.25
HIBCH	PC	2.25
ABHD4	PC	2.25
MFNG	NC & PC	2.25
ABHD3	PC	2.25
B2M	PC	2.25
POMC	NC & PC	2.25
USP18	PC	2.25
TRIM61	NC & PC	2.25
SPON1	PC	2.24
PTAR1	PC	2.24
SPX	PC	2.24
TCF12	PC	2.24
MCM3AP-AS1	PC	2.24
FZD10	PC	2.24
TJP1	PC	2.24
INHBB	PC	2.23
TUBB6	PC	2.23
LEF1	PC	2.23
NPC2	PC	2.23
CHST11	NC & PC	2.23
LIMS1	PC	2.23
SYNE3	PC	2.23
PEAK1	PC	2.23
CNTLN	NC & PC	2.23
RHOQ	NC & PC	2.23
HP	PC	2.22
SMIM30	PC	2.22
SDC2	NC & PC	2.22
SNX29P1	PC	2.22
IFITM4P	PC	2.22
TMPRSS6	NC & PC	2.22
ASXL2	PC	2.22
P4HA1	PC	2.21
PDE3A	NC	2.21
NINL	PC	2.21
RHBDD1	PC	2.21
GDF11	PC	2.21
SNX18	PC	2.21
SMIM10	PC	2.21
DISP1	PC	2.20
HTR2C	NC	2.20
LFNG	PC	2.20

bioRxiv preprint doi: https://doi.org/10.1101/2020.07.17.208132; this version posted July 17, 2020. The copyright holder for this preprint (which was not certified by peer review) is the author/funder, who has granted bioRxiv a license to display the preprint in perpetuity. It is made available under aCC-BY-NC-ND 4.0 International license.

ZNF396	PC	2.20
TBL1X	PC	2.20
DSEL	PC	2.20
ORAI1	PC	2.20
USP3	PC	2.20
CDH23	PC	2.20
BBX	PC	2.19
LINC00467	PC	2.19
CARD8	PC	2.19
VANGL1	PC	2.19
LIX1	PC	2.19
ABCG1	NC & PC	2.19
ZNF260	PC	2.19
CRABP1	NC & PC	2.19
SPATA6	PC	2.18
CD248	PC	2.18
TTF2	PC	2.18
RNF135	PC	2.18
NEXN	NC	2.18
ST3GAL5	NC	2.18
STXBP4	PC	2.18
PLPP4	PC	2.18
MBD2	PC	2.17
IRF7	PC	2.17
SGK1	PC	2.17
TANC1	NC & PC	2.17
ATPAF1	PC	2.17
FAM189A2	PC	2.17
SUCLG2	PC	2.17
RFXANK	PC	2.17
PSKH1	PC	2.17
CYP7B1	NC & PC	2.17
RECQL	PC	2.17
ANTXR1	PC	2.17
FXN	PC	2.16
MPZL1	PC	2.16
PDE9A	PC	2.16
PARD3B	NC & PC	2.16
SLC7A10	PC	2.16
DMAC2L	PC	2.15
TES	NC & PC	2.15
PREX2	NC & PC	2.15
RMDN1	PC	2.15
SEPT10	PC	2.15
DCAF17	PC	2.15
BMP2K	PC	2.15

bioRxiv preprint doi: https://doi.org/10.1101/2020.07.17.208132; this version posted July 17, 2020. The copyright holder for this preprint (which was not certified by peer review) is the author/funder, who has granted bioRxiv a license to display the preprint in perpetuity. It is made available under aCC-BY-NC-ND 4.0 International license.

ARPC1B	PC	2.15
RIT1	PC	2.15
PRTFDC1	PC	2.15
EML4	PC	2.15
MAPRE1	PC	2.15
ZNF710	PC	2.14
FAXDC2	PC	2.14
PDE10A	NC	2.14
ABCB7	PC	2.14
DERA	PC	2.14
NRN1L	NC	2.14
C1orf198	PC	2.14
RELL1	PC	2.13
BDH2	PC	2.13
LAPTM4A	PC	2.13
LOC105274304	NC	2.13
INS-IGF2	PC	2.13
UACA	PC	2.13
HPDL	NC & PC	2.12
ASF1A	PC	2.12
LMO2	NC & PC	2.12
DIPK2B	NC & PC	2.12
CCDC191	PC	2.12
LHFPL2	PC	2.12
SRGN	PC	2.12
ENKUR	PC	2.12
LAYN	PC	2.12
CACFD1	PC	2.12
FBXO30	PC	2.12
CAVIN2	PC	2.11
SOCS6	PC	2.11
TRIM62	PC	2.11
VAT1L	PC	2.11
S100A10	PC	2.10
ENOSF1	PC	2.10
HOMEZ	PC	2.10
STK33	PC	2.10
PTMA	PC	2.10
C11orf65	PC	2.10
ERC1	NC	2.10
SERPINA6	NC & PC	2.10
SPRY3	NC	2.09
B4GALT1	PC	2.09
KCNJ10	PC	2.09
ZNHIT1	PC	2.09
UBL3	PC	2.08

bioRxiv preprint doi: https://doi.org/10.1101/2020.07.17.208132; this version posted July 17, 2020. The copyright holder for this preprint (which was not certified by peer review) is the author/funder, who has granted bioRxiv a license to display the preprint in perpetuity. It is made available under aCC-BY-NC-ND 4.0 International license.

PDE11A	PC	2.08
MTFR1	PC	2.08
ADCY3	NC	2.08
ZNF516	NC & PC	2.08
NOL8	PC	2.08
HTRA1	PC	2.08
UBIAD1	PC	2.08
FAM184B	PC	2.07
CFLAR	PC	2.07
ZNF93	NC & PC	2.07
SUSD2	PC	2.07
SPOCK3	PC	2.07
PTTG1IP	PC	2.07
LRRC1	PC	2.07
NFE2L2	PC	2.06
CTPS2	PC	2.06
ASCC3	PC	2.06
NOS1	NC & PC	2.06
DPF3	PC	2.06
FAM120C	PC	2.06
PTPDC1	NC & PC	2.06
FADS2	PC	2.06
NDST1	PC	2.06
YBX1	PC	2.06
RESP18	NC & PC	2.06
JHY	NC	2.06
ATP6V0E1	PC	2.06
UNC93B1	PC	2.06
THSD4	NC & PC	2.05
FOXF1	PC	2.05
AGPAT3	PC	2.05
ADAM15	PC	2.05
NFIA	PC	2.05
GFRA1	PC	2.04
TGFBR2	PC	2.04
ARHGEF40	PC	2.04
ARL13B	PC	2.04
TGFBR1	PC	2.04
TBL1Y	PC	2.04
NUP93	PC	2.04
TOR4A	PC	2.04
TSPAN12	PC	2.04
GNAL	NC	2.04
SIK3	PC	2.04
NALT1	PC	2.04
PENK	NC	2.04

bioRxiv preprint doi: https://doi.org/10.1101/2020.07.17.208132; this version posted July 17, 2020. The copyright holder for this preprint (which was not certified by peer review) is the author/funder, who has granted bioRxiv a license to display the preprint in perpetuity. It is made available under aCC-BY-NC-ND 4.0 International license.

MTF1	PC	2.04
LINC01869	NC & PC	2.03
EMILIN1	PC	2.03
MOB1A	PC	2.03
LILRB4	PC	2.03
ZBTB20	PC	2.03
TTLL4	PC	2.03
CD302	PC	2.03
PICALM	PC	2.03
NIFK-AS1	PC	2.02
AHCY	PC	2.02
SOX11	PC	2.02
SCP2	PC	2.01
VEGFC	PC	2.01
MED14	PC	2.01
SAR1B	PC	2.01
KANK1	PC	2.01
ZFAND4	PC	2.01
FNDC3A	PC	2.01
LOC100132287	PC	2.01
RPL23AP82	PC	2.01
MOB3A	PC	2.01
MAGT1	PC	2.01
EDEM2	PC	2.00
AP3S2	PC	2.00
YBX3	PC	2.00
G3BP1	PC	2.00
SPACA3	PC	2.00
HBP1	PC	2.00
IFITM2	PC	2.00

bioRxiv preprint doi: https://doi.org/10.1101/2020.07.17.208132; this version posted July 17, 2020. The copyright holder for this preprint (which was not certified by peer review) is the author/funder, who has granted bioRxiv a license to display the preprint in perpetuity. It is made available under aCC-BY-NC-ND 4.0 International license.

Table S10. Novel genes revealed by the DDS to be implicated in DM1 a. Three major brain-functions affected in DM1 are highlighted in relation to synaptic vesicle (VES) recycling and dynamics, and the dopamine (DOP) or serotonin (SER) pathways. The statistical significance (p-value) achieved by the surrogate-data is also shown. Because the list of connector hub genes was obtained from the common genes present in the two cohorts, we only represent here one p-value.

Gene Symbol	*Function*	*p-value*	
Neg-corr genes		1st Cohort	2nd Cohort
CALM3	VES	**0**	**0.0185**
BTBD9	VES	**0**	**0.0206**
STX1A	SER, DOP, VES	**0.0005**	**0.0056**
RAB27B	VES	0.1129	**0.0145**
PCLO	VES	**0.0001**	**0.0113**
BLOC1S6	VES	**0.0076**	**0.0333**
SNAP25	SER, DOP, VES	0.0523	**0.0082**
DOC2A	VES	**0.0022**	**0.0120**
ERC2	VES	**0**	**0.0096**
SYN2	SER, DOP	**0.0018**	**0.0120**
TSPOAP1	SER, DOP	**0**	**0.0198**
Conector-hub genes*			
DNM1L	VES	**0.0236**	
AP2M1	VES	**0.0007**	
SH3GL1	VES	**0**	
DNM1	VES	**0**	
CDK5	VES	**0.0056**	
SH3GL2	VES	**0.0006**	
SYP	VES	**0.0003**	
STXBP1	VES	**0.0013**	
RIMS1	SER, DOP, VES	**0.0003**	
UNC13A	VES	**0**	
RAB3A	SER, DOP, VES	**0**	
APBA2	VES	**0.0003**	
SLC17A7	VES	**0.0002**	
SYT1	SER, DOP, VES	**0**	
AMPH	VES	**0.0002**	
NRN1	VES	**0.0001**	
HTR2A	VES	**0**	
GRIN3A	VES	**0**	
NAPB	VES	**0**	
SYN1	SER, DOP, VES	**0.0069**	

Supplementary References

1. J. D. Brook, et al., Molecular basis of myotonic dystrophy: expansion of a trinucleotide (CTG) repeat at the 3' end of a transcript encoding a protein kinase family member. Cell 68, 799–808 (1992).
2. Y. H. Fu, et al., An unstable triplet repeat in a gene related to myotonic muscular dystrophy. Science 255, 1256–1258 (1992).

bioRxiv preprint doi: https://doi.org/10.1101/2020.07.17.208132; this version posted July 17, 2020. The copyright holder for this preprint (which was not certified by peer review) is the author/funder, who has granted bioRxiv a license to display the preprint in perpetuity. It is made available under aCC-BY-NC-ND 4.0 International license.

3. J. Buxton, et al., Detection of an unstable fragment of DNA specific to individuals with myotonic dystrophy. Nature 355, 547–548 (1992).
4. H. G. Harley, et al., Expansion of an unstable DNA region and phenotypic variation in myotonic dystrophy. Nature 355, 545–546 (1992).
5. M. Mahadevan, et al., Myotonic dystrophy mutation: an unstable CTG repeat in the 3' untranslated region of the gene. Science 255, 1253–1255 (1992).
6. A. Suzuki, et al., MKBP, a novel member of the small heat shock protein family, binds and activates the myotonic dystrophy protein kinase. J. Cell Biol. 140, 1113–1124 (1998).
7. R. S. Savkur, A. V. Philips, T. A. Cooper, Aberrant regulation of insulin receptor alternative splicing is associated with insulin resistance in myotonic dystrophy. Nat. Genet. 29, 40–47 (2001).
8. J. Shin, J. S. Salameh, J. D. Richter, Impaired neurodevelopment by the low complexity domain of CPEB4 reveals a convergent pathway with neurodegeneration. Sci Rep 6, 29395 (2016).
9. G. Ayalon, J. Q. Davis, P. B. Scotland, V. Bennett, An ankyrin-based mechanism for functional organization of dystrophin and dystroglycan. Cell 135, 1189–1200 (2008).
10. K.-Y. Lee, et al., Compound loss of muscleblind-like function in myotonic dystrophy. EMBO Mol Med 5, 1887–1900 (2013).
11. M. Nakamori, et al., Splicing biomarkers of disease severity in myotonic dystrophy. Ann. Neurol. 74, 862–872 (2013).
12. A. Wojtkowiak-Szlachcic, et al., Short antisense-locked nucleic acids (all-LNAs) correct alternative splicing abnormalities in myotonic dystrophy. Nucleic Acids Res. 43, 3318–3331 (2015).
13. R. N. Kanadia, et al., A muscleblind knockout model for myotonic dystrophy. Science 302, 1978–1980 (2003).
14. W. Dansithong, S. Paul, L. Comai, S. Reddy, MBNL1 is the primary determinant of focus formation and aberrant insulin receptor splicing in DM1. J. Biol. Chem. 280, 5773–5780 (2005).
15. M. Nakamori, et al., Aberrant Myokine Signaling in Congenital Myotonic Dystrophy. Cell Rep 21, 1240–1252 (2017).
16. H. Jiang, A. Mankodi, M. S. Swanson, R. T. Moxley, C. A. Thornton, Myotonic dystrophy type 1 is associated with nuclear foci of mutant RNA, sequestration of muscleblind proteins and deregulated alternative splicing in neurons. Hum. Mol. Genet. 13, 3079–3088 (2004).
17. C. Carpentier, et al., Tau exon 2 responsive elements deregulated in myotonic dystrophy type I are proximal to exon 2 and synergistically regulated by MBNL1 and MBNL2. Biochim. Biophys. Acta 1842, 654–664 (2014).
18. A. Annic, et al., Early dopasensitive Parkinsonism related to myotonic dystrophy type 2. Mov. Disord. 23, 2100–2101 (2008).
19. K. Itoh, et al., Neuropathology does not Correlate with Regional Differences in the Extent of Expansion of CTG Repeats in the Brain with Myotonic Dystrophy Type 1. Acta Histochem Cytochem 43, 149–156 (2010).
20. M. Hao, et al., Muscleblind-like 2 (Mbnl2) -deficient mice as a model for myotonic dystrophy. Dev. Dyn. 237, 403–410 (2008).
21. H. Du, et al., Aberrant alternative splicing and extracellular matrix gene expression in mouse models of myotonic dystrophy. Nat. Struct. Mol. Biol. 17, 187–193 (2010).
22. J. E. Morgan, et al., Necroptosis mediates myofibre death in dystrophin-deficient mice. Nat Commun 9, 3655 (2018).
23. M. Wehling-Henricks, et al., Klotho gene silencing promotes pathology in the mdx mouse model of Duchenne muscular dystrophy. Hum. Mol. Genet. 25, 2465–2482 (2016).
24. M. Wehling-Henricks, et al., Macrophages escape Klotho gene silencing in the mdx mouse model of Duchenne muscular dystrophy and promote muscle growth and increase satellite cell numbers through a Klotho-mediated pathway. Hum. Mol. Genet. 27, 14–29 (2018).

bioRxiv preprint doi: https://doi.org/10.1101/2020.07.17.208132; this version posted July 17, 2020. The copyright holder for this preprint (which was not certified by peer review) is the author/funder, who has granted bioRxiv a license to display the preprint in perpetuity. It is made available under aCC-BY-NC-ND 4.0 International license.

25. G. T. Corbett, et al., PrP is a central player in toxicity mediated by soluble aggregates of neurodegeneration-causing proteins. Acta Neuropathol 139, 503–526 (2020).
26. E. Kabashi, et al., TARDBP mutations in individuals with sporadic and familial amyotrophic lateral sclerosis. Nat. Genet. 40, 572–574 (2008).
27. Z. Simmons, What's in the Literature? J Clin Neuromuscul Dis 10, 202–207 (2009).
28. C. A. Boucher, et al., A novel homeodomain-encoding gene is associated with a large CpG island interrupted by the myotonic dystrophy unstable (CTG)n repeat. Hum. Mol. Genet. 4, 1919–1925 (1995).
29. S. K. Heath, S. Carne, C. Hoyle, K. J. Johnson, D. J. Wells, Characterisation of expression of mDMAHP, a homeodomain-encoding gene at the murine DM locus. Hum. Mol. Genet. 6, 651–657 (1997).
30. J. P. Orengo, et al., Expanded CTG repeats within the DMPK 3' UTR causes severe skeletal muscle wasting in an inducible mouse model for myotonic dystrophy. Proc. Natl. Acad. Sci. U.S.A. 105, 2646–2651 (2008).
31. C. Fugier, et al., Misregulated alternative splicing of BIN1 is associated with T tubule alterations and muscle weakness in myotonic dystrophy. Nat. Med. 17, 720–725 (2011).
32. Y. Kino, et al., MBNL and CELF proteins regulate alternative splicing of the skeletal muscle chloride channel CLCN1. Nucleic Acids Res. 37, 6477–6490 (2009).
33. R. Worton, Muscular dystrophies: diseases of the dystrophin-glycoprotein complex. Science 270, 755–756 (1995).
34. M. Naidoo, K. Anthony, Dystrophin Dp71 and the Neuropathophysiology of Duchenne Muscular Dystrophy. Mol Neurobiol 57, 1748–1767 (2020).
35. J. M. Ervasti, K. Ohlendieck, S. D. Kahl, M. G. Gaver, K. P. Campbell, Deficiency of a glycoprotein component of the dystrophin complex in dystrophic muscle. Nature 345, 315–319 (1990).
36. N. Bresolin, et al., Cognitive impairment in Duchenne muscular dystrophy. Neuromuscular Disorders 4, 359–369 (1994).
37. M. Thangarajh, et al., Relationships between DMD mutations and neurodevelopment in dystrophinopathy. Neurology, 10.1212/WNL.0000000000008363 (2019).
38. L. Machuca-Tzili, H. Thorpe, T. E. Robinson, C. Sewry, J. D. Brook, Flies deficient in Muscleblind protein model features of myotonic dystrophy with altered splice forms of Z-band associated transcripts. Hum. Genet. 120, 487–499 (2006).
39. X. Lin, et al., Failure of MBNL1-dependent post-natal splicing transitions in myotonic dystrophy. Hum. Mol. Genet. 15, 2087–2097 (2006).
40. Y. Yamashita, et al., Four parameters increase the sensitivity and specificity of the exon array analysis and disclose 25 novel aberrantly spliced exons in myotonic dystrophy. J. Hum. Genet. 57, 368–374 (2012).
41. Z. Z. Tang, et al., Muscle weakness in myotonic dystrophy associated with misregulated splicing and altered gating of Ca(V)1.1 calcium channel. Hum. Mol. Genet. 21, 1312–1324 (2012).